

1 Broadening the Message: A Nanovaccine Co-  
2 loaded with Messenger RNA and  $\alpha$ -GalCer Induce  
3 Antitumor Immunity Through Conventional and  
4 Natural Killer T Cells

5 *Rein Verbeke<sup>†</sup>, Ine Lentacker<sup>†</sup>, Karine Breckpot<sup>‡</sup>, Jonas Janssens<sup>§</sup>, Serge Van Calenbergh<sup>§</sup>,*  
6 *Stefaan C. De Smedt<sup>\*†#</sup>, and Heleen Dewitte<sup>‡#</sup>*

7 <sup>†</sup> Ghent Research Group on Nanomedicines, Faculty of Pharmacy & Cancer Research Institute  
8 Ghent (CRIG), Ghent University Hospital, Ghent University, Ghent, Belgium

9 <sup>‡</sup> Laboratory of Molecular and Cellular Therapy, Department of Biomedical Sciences, Vrije  
10 Universiteit Brussel (VUB), Jette, Belgium

11 <sup>§</sup> Laboratory for Medicinal Chemistry, Faculty of Pharmacy, Ghent University, Ghent,  
12 Belgium

13

14 # Senior authors contributed equally to this work.

15

16 KEYWORDS: iNKT cells, T cell, mRNA vaccine, nanoparticle, checkpoint inhibition,  $\alpha$ -  
17 Galactosylceramide, modified nucleotides

18

1 ABSTRACT: Messenger RNA encoding tumor antigens has the potential to evoke effective  
2 antitumor immunity. This study reports on a nanoparticle platform, named mRNA Galsomes,  
3 that successfully co-delivers nucleoside-modified antigen-encoding mRNA and the glycolipid  
4 antigen and immunopotentiator  $\alpha$ -Galactosylceramide ( $\alpha$ -GC) to antigen-presenting cells after  
5 intravenous administration. By co-formulating low doses of  $\alpha$ -GC, mRNA Galsomes induce a  
6 pluripotent innate and adaptive tumor-specific immune response in mice, with invariant  
7 natural killer T cells (iNKT) as a driving force. In comparison, mRNA Galsomes exhibit  
8 advantages over the state of the art cancer vaccines using unmodified ovalbumin (OVA)-  
9 encoding mRNA, as we observed up to seven times more tumor-infiltrating antigen-specific  
10 CTLs, combined with a strong iNKT cell and NK cell activation. In addition, the presence of  
11 suppressive myeloid cells (myeloid-derived suppressor cells and tumor-associated  
12 macrophages) in the tumor micro-environment was significantly lowered. Owing to these  
13 antitumor effects, OVA mRNA Galsomes significantly reduced tumor growth in established  
14 E.G7-OVA lymphoma, with a complete tumor rejection in 40% of the animals. Moreover,  
15 therapeutic vaccination with mRNA Galsomes enhanced the responsiveness to treatment with  
16 a PD-L1 checkpoint inhibitor in B16-OVA melanoma, as evidenced by a synergistic reduction  
17 of tumor outgrowth and a significantly prolonged median survival. Taken together, these data  
18 show that intravenously administered mRNA Galsomes can provide controllable, multi-  
19 faceted and effective antitumor immunity, especially when combined with checkpoint  
20 inhibition.

21

1 Where for long the use of mRNA was limited due to its perceived instability, it is nowadays  
2 possible to successfully deliver mRNA *in vivo*.<sup>1</sup> This is strongly supported by two recent  
3 breakthroughs: (i) the packaging of mRNA molecules inside nanoparticles, designed to  
4 improve the selective cell targeting and cytosolic delivery of mRNA<sup>2-9</sup> and (ii) the technical  
5 progress in the mRNA construct, including the incorporation of modified nucleotides,  
6 yielding more stable mRNA with an improved translation capacity.<sup>10-13</sup> Particularly in the  
7 field of vaccination, mRNA encoding antigens has emerged as a versatile and promising  
8 platform.<sup>14</sup> Preclinical studies and first clinical trials with mRNA-based vaccines have shown  
9 to afford protective humoral responses, as well as strong cellular responses against diverse  
10 diseases.<sup>5, 15, 16</sup>

11 In the field of cancer immunotherapy, Kranz *et al.* provided first-in-human proof that by  
12 targeting mRNA lipid nanoparticles (LNPs) to dendritic cells (DCs), cytotoxic T cell (CTL)  
13 responses were induced against the encoded tumor antigens.<sup>5</sup> They and others demonstrated  
14 that besides the successful mRNA expression by DCs, the mode of action of mRNA vaccines  
15 largely depends on the induction of type I interferon (IFN).<sup>6, 17-19</sup> More specifically, upon  
16 cellular entry, mRNA molecules trigger innate immune activation pathways, including the  
17 endosomal Toll-like receptor (TLR)-7 and cytosolic receptors MDA-5 (melanoma  
18 differentiation-associated protein 5) and RIG-I (retinoic acid-inducible gene I), which results  
19 in type I IFN signaling and the induction of an antiviral immune response. Importantly,  
20 virtually all mRNA vaccines in clinical development rely on this inherent self-adjuvant effect  
21 of mRNA. However, it was shown that type I IFN signaling acts as a double-edged sword as  
22 the evoked immune response prematurely stops mRNA-translation, thereby lowering antigen  
23 bioavailability.<sup>20, 21</sup> Moreover, it was suggested that type I IFN, depending on the relative  
24 timing to T cell priming, can either positively or negatively affect T cell responses, with pre-  
25 exposure to type I IFN resulting in T cell exhaustion and apoptosis.<sup>22, 23</sup> In addition, high

1 levels of IFN- $\alpha$  can induce adverse effects ranging from flu-like symptoms to autoimmune  
2 sequelae and even life-threatening events.<sup>24, 25</sup>

3 Besides issues related to vaccine-induced type I IFN secretion, the current mRNA vaccines  
4 often fall short to evoke durable antitumor immunity. Indeed, while mRNA-based cancer  
5 vaccines show optimal properties for the activation of cytotoxic T lymphocyte (CTL)  
6 responses, such as the preferential antigen presentation *via* MHC-I molecules and the  
7 activation of type I IFN-dependent immunity, the evoked immunity is generally counteracted  
8 by a plethora of tumor-mediated immunosuppressive mechanisms. First of all, tumor cells  
9 may have an impaired or deficit presentation of antigens, making them invisible to CTLs.<sup>26</sup>  
10 Additionally, during an immune attack and as a result of the production of interferons,  
11 immune checkpoint pathways are activated as mechanisms to resist adaptive immunity, such  
12 as the expression of programmed cell death 1 (PD-1) ligand (PD-L1) by tumor cells, antigen-  
13 presenting cells (APCs) and its receptor PD-1 on the effector cells.<sup>27-29</sup> Moreover, tumor-  
14 infiltrating CTLs have to deal with immune resistance mediated by various suppressive cells,  
15 including alternatively activated M2 macrophages, myeloid derived suppressor cells  
16 (MDSCs) and regulatory T cells.<sup>30</sup> Thus, ideally, mRNA vaccines should not solely focus on  
17 the activation of CTLs, but should more broadly harness the host's immune system to tackle  
18 these different suppressive mechanisms.

19 To address these issues, continued research is required to develop more safe mRNA vaccines,  
20 while further improving their effectiveness for cancer immunotherapy. Here, we propose an  
21 mRNA nanovaccine, which explores the combined delivery of immunosilent, nucleoside-  
22 modified mRNA and the glycolipid  $\alpha$ -galactosylceramide ( $\alpha$ -GC), to achieve broad and  
23 durable, but controllable and effective antitumor immunity.

1 By using mRNA containing pseudouridine ( $\Psi$ ) and 5-methylcytidine (5meC), we choose to  
2 minimize the immune recognition of mRNA and associated anti-mRNA mechanisms and  
3 toxicity issues. As such, we have previously established a liposomal formulation for mRNA  
4 delivery, composed of DOTAP (1,2-dioleoyl-3-trimethylammonium-propane) and cholesterol,  
5 efficiently targeting DCs after intravenous (i.v.) administration. By using nucleoside-  
6 modified mRNA, we obtained highly improved mRNA expression levels, while strongly  
7 reducing the release of type I IFN.<sup>31</sup>

8 In addition, we hypothesized that instead of inducing type I IFN responses, pairing  
9 nucleoside-modified mRNA with  $\alpha$ -GC could hold numerous appealing features for cancer  
10 immunotherapy.  $\alpha$ -GC is a well-known glycolipid antigen that, when presented by the MHC-  
11 I-like molecule CD1d on APCs, leads to the potent activation of invariant natural killer T cells  
12 (iNKT). This subset of unconventional T cells contributes to innate and adaptive immunity,  
13 but can also exert direct and indirect antitumor effects.<sup>32-34</sup> Unlike the classical immune  
14 adjuvants that directly trigger danger pathways,  $\alpha$ -GC exerts an indirect adjuvant effect  
15 through the bidirectional interaction between  $\alpha$ -GC-presenting DCs and iNKT cells.<sup>35</sup> As  
16 such, iNKT cells can activate DCs through the interaction between CD40 and CD40 ligand,  
17 evoking the production of cytokines (*e.g.*, IL-12p70) and expression of co-stimulatory  
18 receptors (*e.g.*, CD80, CD86, and CD70). In turn, when activated, iNKT cells proliferate and  
19 secrete a wide range of cytokines (*e.g.*, IL-2, IFN- $\gamma$ , IL-4 and TNF- $\alpha$ ), which further promotes  
20 the recruitment and activation of DCs, B cells, and T cells. Furthermore, iNKT cells are  
21 known to induce the down-stream activation of NK cells, to exhibit direct tumor killing  
22 effects (*e.g.*, *via* CD1d recognition) and have been shown to positively modulate tumor-  
23 associated macrophages (TAMs) and MDSCs in the tumor microenvironment.<sup>36-39</sup>

24 In order to efficiently co-deliver nucleoside-modified mRNA and the iNKT ligand  $\alpha$ -GC, we  
25 developed a nanoformulation, which will be referred to as “mRNA Galsomes”. The potential

1 of this formulation was evaluated by investigating its adjuvancy, the activation of antigen-  
2 specific T cell responses, NK- and iNKT cells, and therapeutic effectiveness in two tumor  
3 models. Importantly, the i.v. delivery of mRNA Galsomes was compared to the current “gold  
4 standard” in mRNA vaccination, which is currently under clinical investigation and consists  
5 of LNPs loaded with immunogenic (unmodified) mRNA and therefore rely on the mRNA’s  
6 self-adjuvancity and corresponding type I IFN to drive immunity.<sup>5</sup> Finally, we evaluated if  
7 we could further improve the therapeutic outcome by co-administering checkpoint inhibitors  
8 (anti-PD-L1 antibody) to enhance CTL responses and prevent the induction of adaptive  
9 resistance (see **Graphical Table of Contents**).

## 10 RESULTS

### 11 **mRNA Galsomes: DOTAP-cholesterol liposomes as delivery agent for nucleoside-** 12 **modified mRNA and $\alpha$ -GC**

13 Previously, we succeeded in developing a liposomal formulation for i.v. injection composed  
14 of DOTAP and cholesterol, that can be used to complex mRNA and retains its full transfection  
15 potential in serum.<sup>31</sup> DOTAP/cholesterol LNPs loaded with mRNA remain intact in  
16 biologically relevant media, as shown by a stable particle size when incubated in human  
17 serum for up to 24h, and ensure a durable protection of the mRNA cargo from degradation. A  
18 schematic representation of mRNA Galsomes is shown in **Figure 1A**. We demonstrate that  
19 the physicochemical properties of mRNA Galsomes containing 1 mol% of  $\alpha$ -GC were  
20 unaltered compared to mRNA LNPs formulated without  $\alpha$ -GC, with a mean size of 190 nm  
21 and a zeta potential of +47 mV (**Figure 1B**).

22 By co-formulating the  $\alpha$ -GC and the antigen-encoding mRNA in a single nanoparticle system,  
23 it is possible to achieve simultaneous delivery of both components to the same DCs, thus  
24 ensuring optimal synchronization between the interactions of the particle-laden DCs with

1 CD8<sup>+</sup> T cells on one hand, and the iNKT cells on the other hand. In this regard, it is important  
2 to note that both nanoparticle cargos, mRNA and  $\alpha$ -GC, have different requirements regarding  
3 their intracellular delivery. mRNA should escape from the endosomes to the cytoplasm to  
4 allow adequate antigen synthesis by the ribosomes. By contrast,  $\alpha$ -GC must accumulate in late  
5 endosomes and lysosomes of DCs, where it is loaded on CD1d molecules and presented to  
6 iNKT cells. As such, we first estimated the delivery efficiency for both mRNA and  $\alpha$ -GC,  
7 using DOTAP-cholesterol liposomes as carrier system, and assessed whether or not the  
8 immune response that occurs upon  $\alpha$ -GC presentation to iNKT cells affects the mRNA  
9 expression levels.

10 To evaluate  $\alpha$ -GC delivery, bone marrow-derived DCs (BM-DCs) were incubated either with  
11  $\alpha$ -GC alone (dissolved in DMSO) or mRNA Galsomes (containing equal doses of  $\alpha$ -GC).  
12 When using BODIPY-labeled  $\alpha$ -GC, it was clear that the intracellular delivery of  $\alpha$ -GC was  
13 up to ten times higher by the delivery *via* mRNA Galsomes (**Figure 1C**). This was confirmed  
14 by representative confocal microscopy images of BM-DCs after uptake of BODIPY-labeled  
15  $\alpha$ -GC, either by incubation of the cells with  $\alpha$ -GC alone or  $\alpha$ -GC formulated in mRNA  
16 Galsomes (**Supplementary Figure S1**). This also translated into an enhanced presentation of  
17  $\alpha$ -GC by CD1d: we observed a threefold increase in the presentation of  $\alpha$ -GC *via* CD1d  
18 complexes compared to  $\alpha$ -GC alone (**Figure 1D**).

19 To determine the potency of mRNA Galsomes to initiate an immune response, we performed  
20 a dose-response study by injecting mice i.v. with mRNA Galsomes containing a fixed dose of  
21 10  $\mu$ g mRNA and decreasing doses of  $\alpha$ -GC (**Figure 1E**). Twelve hours post-injection, iNKT  
22 cell activation was measured indirectly by quantifying the levels of IFN- $\gamma$  in serum. When  
23 injecting mRNA Galsomes containing 1.4  $\mu$ g  $\alpha$ -GC, a dose which corresponds to the amount  
24 of  $\alpha$ -GC that is typically administered systemically in mice, levels of IFN- $\gamma$  up to 25 000  
25 pg ml<sup>-1</sup> could be detected in serum.<sup>35</sup> Although this indicates that mRNA Galsomes are very

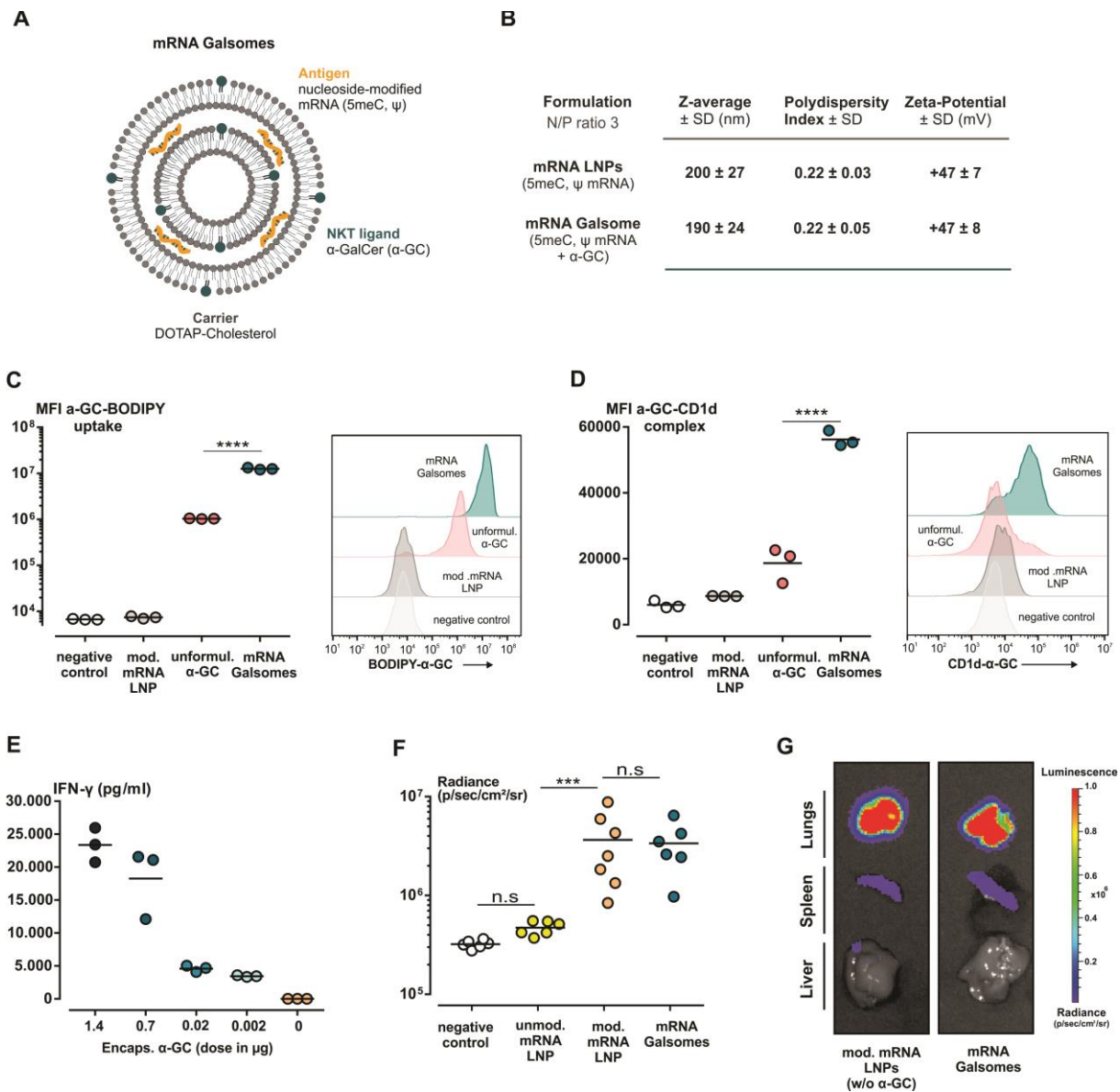
1 potent to induce immune responses, this coincided with splenomegaly in all of the animals.  
2 However, the levels of IFN- $\gamma$  could easily be refined by dose adjustments of  $\alpha$ -GC.  
3 Importantly, when drastically lower doses were used, down to 20 ng  $\alpha$ -GC per mouse (or  
4 0.015 mol% of the total amount of lipids in the nanoparticle), this still resulted in high levels  
5 of IFN- $\gamma$  ( $\sim$ 4000 pg ml<sup>-1</sup>), but without any signs of acute toxicity. Therefore, we used mRNA  
6 Galsomes packaging 20 ng of  $\alpha$ -GC for further experiments.

7 Previous attempts where mRNA was combined with other adjuvants have raised compatibility  
8 issues, since DC maturation can prematurely abrogate cellular uptake mechanisms (*e.g.*,  
9 macropinocytosis) or potentially induce anti-mRNA defense mechanisms (*e.g.*, type I IFN  
10 signaling) leading to fast mRNA degradation.<sup>40, 41</sup> For these reasons we investigated the  
11 impact of  $\alpha$ -GC inclusion on mRNA translation. Firstly, *in vitro* experiments in murine BM-  
12 DCs as well as human monocyte-derived DCs demonstrated that mRNA Galsomes could  
13 efficiently transfect both cell types with eGFP-encoding mRNA in serum-containing medium  
14 (**Supplementary Figure S2**). In addition, we performed transfection experiments in mice,  
15 using mRNA encoding firefly luciferase (fLuc) as reporter gene. Mice were injected i.v. with  
16 nanoparticles encapsulating different cargos; (i) unmodified mRNA (unmod. mRNA LNPs),  
17 (ii) nucleoside-modified mRNA alone (mod. mRNA LNPs), or (iii) nucleoside-modified  
18 mRNA combined with  $\alpha$ -GC (mRNA Galsomes). Bioluminescence was evaluated 6h later.  
19 **Figures 1F-G** demonstrate that incorporation of  $\alpha$ -GC did not interfere with the translation of  
20 mRNA in lungs and spleen, and that increasing mRNA doses up to 10  $\mu$ g per animal, resulted  
21 in a higher protein expression in the lungs and spleen (**Supplementary Figure S3**).

22 As expected, nanoparticles containing unmodified fLuc mRNA display significantly lower  
23 expression levels, which results from their lower intracellular stability, as well as from type I  
24 IFN-mediated antiviral pathways programmed to degrade and avoid the translation of  
25 mRNA.<sup>41</sup> Together, these results indicate that co-packaging of nucleoside-modified mRNA



1 and  $\alpha$ -GC improves  $\alpha$ -GC delivery and presentation, without affecting the mRNA expression  
 2 levels.



3  
 4 **Figure 1.** mRNA Galsomes promote the delivery of  $\alpha$ -GC to DCs without affecting mRNA  
 5 transfection. (A) Schematic representation of a nanoparticle consisting of DOTAP-cholesterol  
 6 LNPs, nucleoside-modified mRNA (5meC,  $\psi$ ) and the NKT ligand  $\alpha$ -GC. (B) Size (Z  
 7 average), polydispersity index (PdI) and zeta potential of mRNA LNPs dispersed in HEPES  
 8 buffer, formulated with or without  $\alpha$ -GC (*i.d.* 1 mol% of total lipids,  $n=3$ ). A quantitative  
 9 flow cytometric analysis of the increase in intracellular delivery of BODIPY-labeled  $\alpha$ -GC

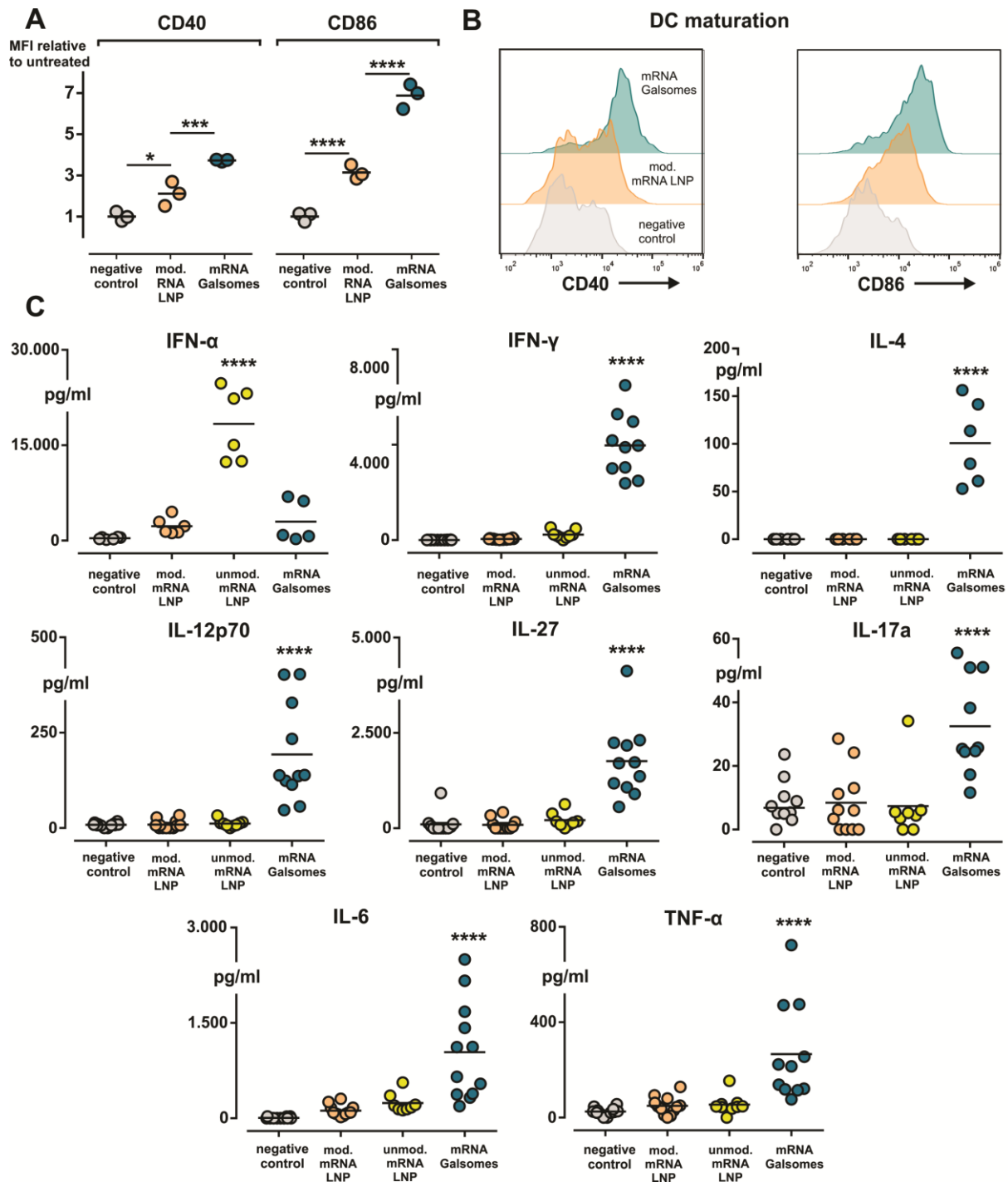
1 formulated in mRNA Galsomes is shown in (C), where untreated cells served as negative  
2 controls. (D) Enhanced surface presentation of  $\alpha$ -GC in CD1d complexes by BM-DCs 24h  
3 after incubation with  $\alpha$ -GC in mRNA Galsomes. (panels C-D show representative data of  
4 three independent experiments, untreated cells serve as negative controls). (E) Dose-response  
5 experiment: IFN- $\gamma$  levels in serum of C57BL/6 mice 12h after i.v. injection of mRNA  
6 Galsomes containing decreasing doses of  $\alpha$ -GC. (F) Graph summarizing whole-body  
7 expression levels of fLuc mRNA in C57Bl/6 mice 6h after i.v. injection of nanoparticles  
8 containing different cargos, or PBS (negative control); liposomes containing unmodified  
9 mRNA, nucleoside-modified- or nucleoside-modified mRNA nanoparticles formulated with  
10  $\alpha$ -GC ( $n=6-7$ , pooled from two independent experiments) (G) Representative  
11 bioluminescence images of isolated organs (lungs, spleen and liver). For all these  
12 experiments, mRNA encoding fLuc was used. Statistical analyses on datasets were performed  
13 by One-Way ANOVA followed by Turkey's post hoc test. Asterisks indicate statistical  
14 significance (n.s.,  $p > 0.05$ ; \*\*\*,  $p < 0.001$ ; \*\*\*\*,  $p < 0.0001$ ).

### 15 **mRNA Galsomes mediate strong adjuvant effects and activate dendritic cells *in vivo***

16 Immune activation by  $\alpha$ -GC is an indirect phenomenon: DCs that present  $\alpha$ -GC by CD1d will  
17 stimulate iNKT cells, which, in turn, cause phenotypic maturation of DCs by CD40-CD40-  
18 ligand interaction. To assess if this is also the case for mRNA Galsomes, especially with the  
19 low (20 ng)  $\alpha$ -GC doses used, we investigated the maturation status of splenic DCs 24h after  
20 particle injection (**Figure 2A-B**). We could observe a strong and significant up-regulation of  
21 the activation markers CD40 and CD86 on splenic DCs of mice treated with mRNA  
22 Galsomes, relative to untreated mice and mice injected with LNPs containing nucleoside-  
23 modified mRNA without  $\alpha$ -GC. Importantly, no DC maturation was observed when mRNA  
24 Galsomes were added to BM-DC cultures *in vitro*, in the absence of iNKT cells. This

1 indicates that this *in vivo* maturation effect was mediated by the ligation with iNKT cells  
2 **(Supplementary Figure S4).**

3 To investigate the immune response in more detail, a broad screening of inflammatory  
4 cytokines was performed in blood of animals 6h after vaccination (**Figure 2C**). As expected,  
5 nanoparticles containing unmodified mRNA induced a strong release of IFN- $\alpha$ , while this was  
6 not the case with nucleoside-modified mRNA nanoparticles (with or without  $\alpha$ -GC). By  
7 contrast, mRNA Galsomes induced a pronounced production of IFN- $\gamma$  and IL-4. What is  
8 more, in the group receiving mRNA Galsomes, we could also detect the presence of T cell-  
9 stimulating cytokines, such as IL-12p70 and IL-27, and elevated levels of IL-6, TNF $\alpha$  and IL-  
10 17. Importantly, this broad spectrum of cytokines did not induce visible toxicity symptoms  
11 (changes in body condition score, behavior, global appearance or posture) and no pathological  
12 changes were identified in H&E stained organ sections of lungs, spleen and liver, while  
13 normal levels of ALT activity were measured (**Supplementary Figure S5**).



1

2 **Figure 2.** mRNA Galsomes containing low doses of  $\alpha$ -GC (20 ng) induce the maturation of  
 3 dendritic cells *in vivo* and stimulate the release of immunostimulatory cytokines. (A) Splenic  
 4 DCs (CD11c<sup>+</sup>) showed an increase in the expression of the activation markers CD40 and  
 5 CD86 (expressed as a fold change in MFI) 24h after administration of mRNA Galsomes,  
 6 while incomplete maturation was observed with nanoparticles containing nucleoside-modified

1 mRNA alone ( $n=4$ ). **(B)** Representative histograms of CD40 and CD86 expression by CD11c<sup>+</sup>  
2 cells. **(C)** Serum samples were collected at 6h post-injection and screened for the release of  
3 inflammatory cytokines: while nanoparticles containing unmodified mRNA trigger the  
4 production of IFN- $\alpha$ , mRNA Galsomes induce distinct cytokine responses, including IFN- $\gamma$ ,  
5 IL-4, IL-12p70, IL-27, IL-17a, IL-6 and TNF- $\alpha$ . For all experiments in this figure, fLuc  
6 mRNA was used. Data are pooled from at least two independent experiments. Mice injected  
7 with PBS serve as negative controls. Statistical analyses on datasets were performed by One-  
8 Way ANOVA followed by Turkey's post hoc test. Asterisks indicate statistical significance  
9 compared to negative control (\*\*\*\*,  $p < 0.0001$ ).

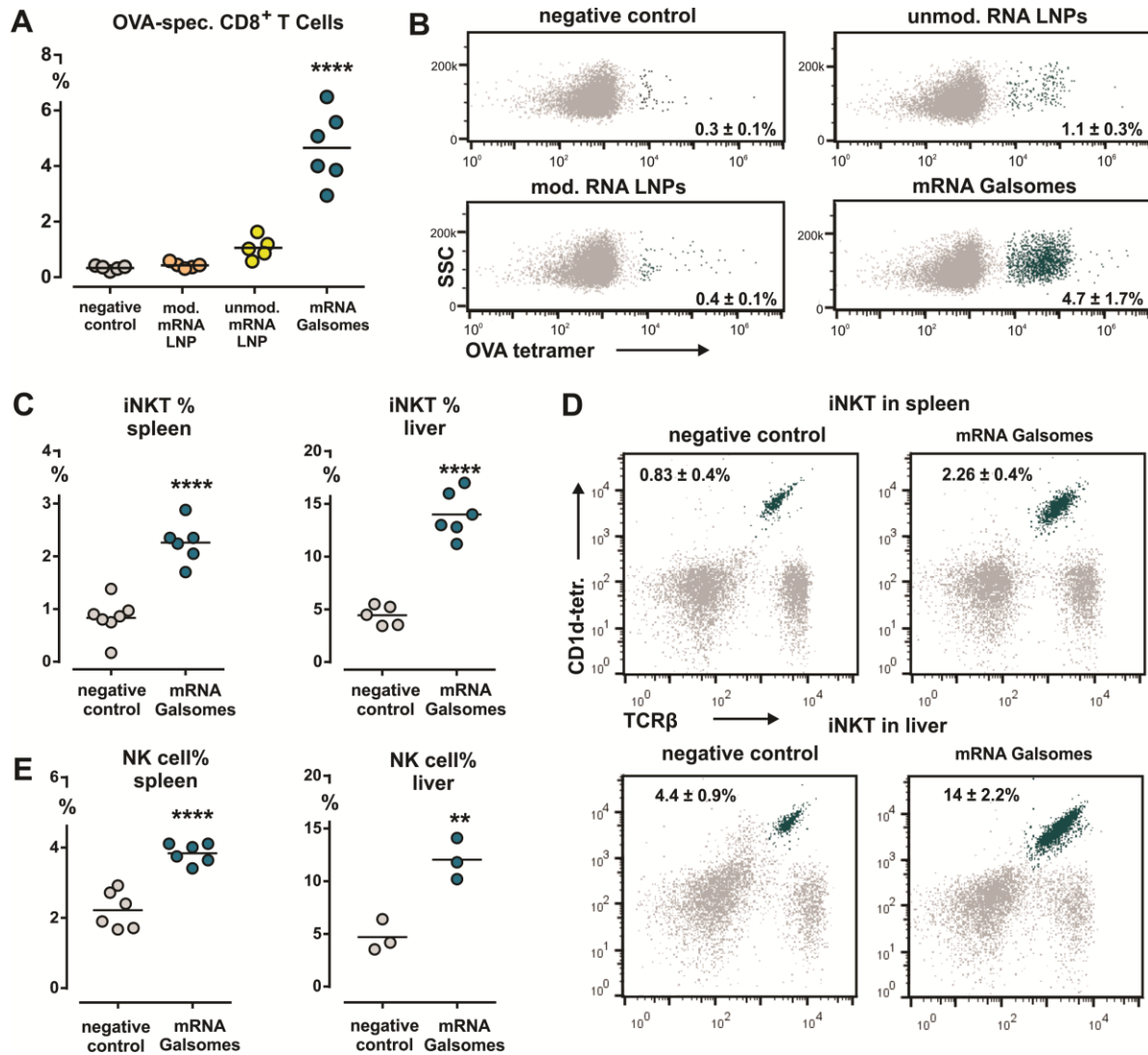
#### 10 **mRNA Galsomes as pluripotent inducers of immunity**

11 One could expect that the increased mRNA expression levels combined with strong DC  
12 maturation, and the production of CTL-inducing cytokines such as IL-12p70, hold potential  
13 for mRNA Galsomes to compete with type I IFN-dependent mRNA vaccines. In addition to T  
14 cell-mediated immunity, the combination with  $\alpha$ -GC could also offer the advantage of  
15 activating both iNKT- and NK cells shaping a broader and potentially synergistic antitumor  
16 immunity.

17 To evaluate these multiple effector responses, animals were immunized with mRNA encoding  
18 chicken ovalbumin (OVA) as a model antigen. Six days after immunization, cell numbers of  
19 OVA-specific CTLs were measured in isolated spleens (**Figure 3A-B**). Interestingly, we  
20 observed that mRNA Galsomes generated four to five times higher levels of OVA-specific  
21 CTLs compared to mice treated with nanoparticles containing unmodified OVA mRNA.

22 To evaluate the proliferation of iNKT and down-stream NK cell responses, spleen and liver  
23 were isolated three days after vaccination. Corresponding to the cytokine responses (**Figure**  
24 **2B**), we observed an increased proliferation of iNKT cells, from 0.8 to 2.3% in spleen and 4.4

1 to 14% in liver (**Figure 3C-D**). Accordingly, mRNA Galsomes also mediated the  
 2 proliferation of NK cells as their levels increased from 2.2 to 3.8 % and 4.7 to 12%, in spleen  
 3 and liver, respectively. (**Figure 3E**).



4  
 5 **Figure 3.** mRNA Galsomes mediate pluripotent innate and adaptive immune responses. (**A**)  
 6 mRNA Galsomes strongly mediate the induction of antigen-specific CD8<sup>+</sup> T cell responses.  
 7 Mice were immunized with OVA mRNA LNPs. Six days later, percentages of OVA-specific  
 8 splenic CD8<sup>+</sup> T cells were measured using an H-2kb OVA tetramer staining. (**B**)  
 9 Representative flow cytometry scatter plots of OVA-specific CD8<sup>+</sup> T cells. Blue events  
 10 represent tetramer-stained CD8<sup>+</sup> cells. (**C**) Three days post-injection of mRNA Galsomes,

1 spleen and liver displayed expanded iNKT cell numbers compared to untreated mice. **(D)**  
2 Representative flow plots of iNKT cells in spleen and liver (Blue events indicate TCR $\beta^+$ ,  
3 mCD1d PBS-57 $^+$  cells). **(E)** Down-stream activation of NK cells (CD3 $^-$ , NK1.1 $^+$  cells). The  
4 data in this figure ( $n=6$ ) are pooled from two independent experiments. PBS-injected mice  
5 serve as negative controls. Statistical analyses on datasets were performed by One-Way  
6 ANOVA followed by Turkey's post hoc test for (A). Pairwise comparisons in sections (C)  
7 and (E) were performed *via* a student's t test. Asterisks indicate statistical significance (\*\*,  $p$   
8  $< 0.01$ ; \*\*\*\*,  $p < 0.0001$ ).

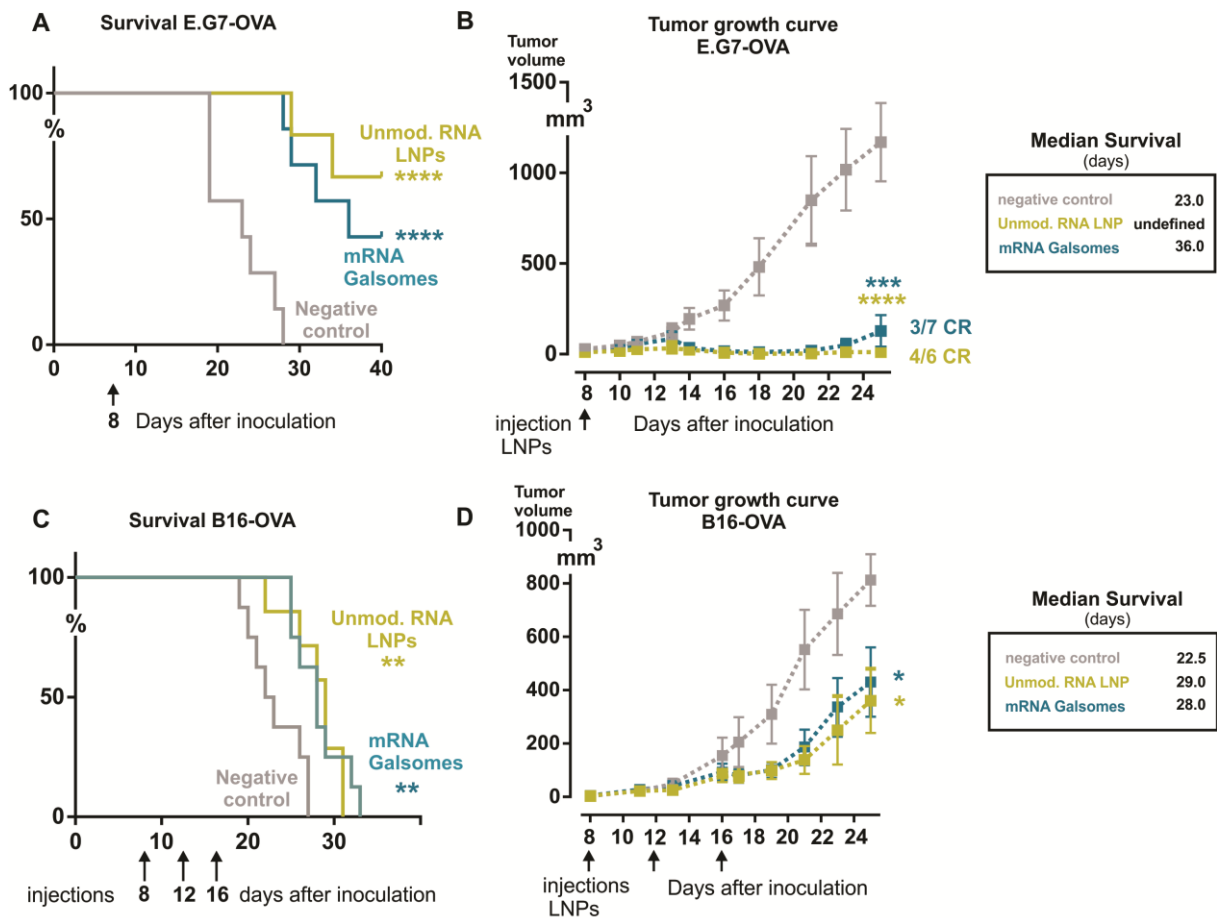
## 9 **Therapeutic efficacy of mRNA Galsomes in E.G7-OVA lymphoma- and B16-OVA** 10 **melanoma**

11 To assess the potential of mRNA Galsomes in a therapeutic vaccination study, mice were  
12 subcutaneously inoculated with OVA-expressing E.G7 lymphoma cells or B16-OVA  
13 melanoma cells and vaccinated when tumors were palpable at day 8 with mRNA encoding  
14 OVA.

15 E.G7-OVA bearing mice were treated with a single administration of either mRNA Galsomes  
16 or nanoparticles containing unmodified mRNA, in order to differentiate between the  
17 therapeutic potential of nanoparticles that evoke immunity based on iNKT cell activation or a  
18 type I IFN response, respectively. First of all, both therapies resulted in a significant reduction  
19 in tumor growth and prolonged survival, relative to untreated mice (**Figure 4A-B**). Overall,  
20 mice treated with nanoparticles containing unmodified mRNA, showed complete tumor  
21 regression in 4/6 animals, and treatment with mRNA Galsomes resulted in complete tumor  
22 regression in 3/7 animals, and no significant differences could be observed in tumor growth  
23 between both treatment groups. It should be noted that nucleoside-modified mRNA

1 nanoparticles without  $\alpha$ -GC did not have significant effects on tumor growth  
 2 (Supplementary Figure S6).

3 In a more aggressive B16-OVA melanoma model, animals received three administrations of  
 4 either mRNA Galsomes or unmodified mRNA nanoparticles on day 8, day 12 and day 16 after  
 5 tumor inoculation. Although we observed a delay of tumor outgrowth, there was only a  
 6 modest prolongation of survival for mice treated with mRNA Galsomes or nanoparticles  
 7 containing unmodified mRNA, with median survival of 28 days and 29 days, respectively,  
 8 compared to 22.5 days for untreated animals (Figure 4C-D). In addition, we noticed that  
 9 multiple doses could not efficiently boost or prolong the antitumor responses. This also  
 10 occurred in the E.G7-OVA model, where a second (boost) vaccination did not result in better  
 11 control of tumor outgrowth (Supplementary Figure S7).



12



1 **Figure 4.** Therapeutic vaccination with OVA mRNA Galsomes or nanoparticles containing  
2 unmodified OVA mRNA in E.G7-OVA lymphoma and B16-OVA melanoma model. Mice  
3 were subcutaneously inoculated with E.G7-OVA cells or B16-OVA cells ( $3 \times 10^5$  cells). E.G7-  
4 OVA bearing mice were vaccinated on day 8 when tumors were clearly visible. B16-OVA  
5 bearing mice received three vaccinations on day 8, day 12 and day 16. Graphs show Kaplan–  
6 Meier survival curves in E.G7-OVA model (**A**) and B16-OVA model (**C**), and the respective  
7 tumor growth curves (**B and D**) as a function of time for an untreated control group (negative  
8 control), and for mice treated with OVA mRNA Galsomes or nanoparticles containing  
9 unmodified OVA mRNA ( $n=7-8$ ). Statistical analysis on the survival curves (A) and (C) was  
10 performed using a log-rank (Mantel–Cox) test. In (B) and (D), tumor volumes measured at  
11 day 25 were compared by a One-way ANOVA followed by Tukey's post hoc test. Asterisks  
12 indicate statistical significance compared to the untreated group (\*  $p < 0.05$ ; \*\*,  $p < 0.01$ ; \*\*\*,  
13  $p < 0.001$ ; \*\*\*\*  $p < 0.0001$ )

14 **mRNA Galsomes promote the tumor infiltration of CTLs, iNKT cells and NK cells, but**  
15 **immune surveillance is hampered by the PD-1/PD-L1 axis**

16 Since complete control of tumor outgrowth was not achieved, we aimed to investigate which  
17 immune suppressive mechanisms might be at play to counteract the evoked antitumor  
18 immunity by mRNA Galsomes or nanoparticles containing unmodified mRNA. Therefore,  
19 experiments were performed where B16-OVA bearing mice were euthanized two days after a  
20 second nanoparticle administration (day 14), and a detailed analysis of the tumor immune  
21 microenvironment was performed. Tumor and spleen were screened for effector responses  
22 and/or suppressive mechanisms that could impact the therapeutic outcome. The most  
23 important findings are shown in **Figure 5**. The flow cytometry gating strategy for each cell  
24 type can be found in **Supplementary Figure S8**.

1 First of all, animals treated with mRNA Galsomes exhibited up to five times higher levels of  
2 tumor infiltrating OVA-specific CTLs, whereas CTL presence at the tumor site merely  
3 doubled after vaccination with nanoparticles containing unmodified mRNA compared to the  
4 untreated group (**Figure 5A**). Likewise, vaccinations with mRNA Galsomes resulted in six to  
5 seven times higher numbers of CTLs specific for OVA (10% of viable cells in tumor, as  
6 determined by SIINFEKL-H2Kb tetramer staining) compared to animals treated with  
7 nanoparticles containing unmodified mRNA, while almost no (< 0.04 %) OVA-specific CTLs  
8 were detected in the tumors of the untreated animals (**Figure 5B**). In addition, we detected a  
9 fourfold increase in iNKT cell numbers in the tumors of mice treated with mRNA Galsomes,  
10 compared to the other groups (**Figure 5C**). For both treatments, increased levels of tumor-  
11 infiltrating NK cells were observed, with  $\pm$  13% NK cells for mRNA Galsomes and  $\pm$  11%  
12 NK cells for nanoparticles containing unmodified mRNA compared to untreated mice with  
13 only  $\pm$  5% NK cells (**Figure 5D**). By analyzing the tumor site for suppressive immune cells,  
14 we found that the delivery of unmodified mRNA resulted in a twofold increase in MDSCs  
15 (CD11b<sup>+</sup>, GR1<sup>+</sup>, MHC-II<sup>-</sup> cells) compared to untreated controls. Interestingly, this rise in  
16 MDSC levels was not observed in animals treated with mRNA Galsomes (**Figure 5E**).  
17 Furthermore, we noticed that almost all TAMs (CD11b<sup>+</sup>, F4/80<sup>+</sup> cells) in the mRNA  
18 Galsome-group displayed a pro-inflammatory M1-like phenotype, marked by increased levels  
19 of MHC-II (**Figure 5F**).

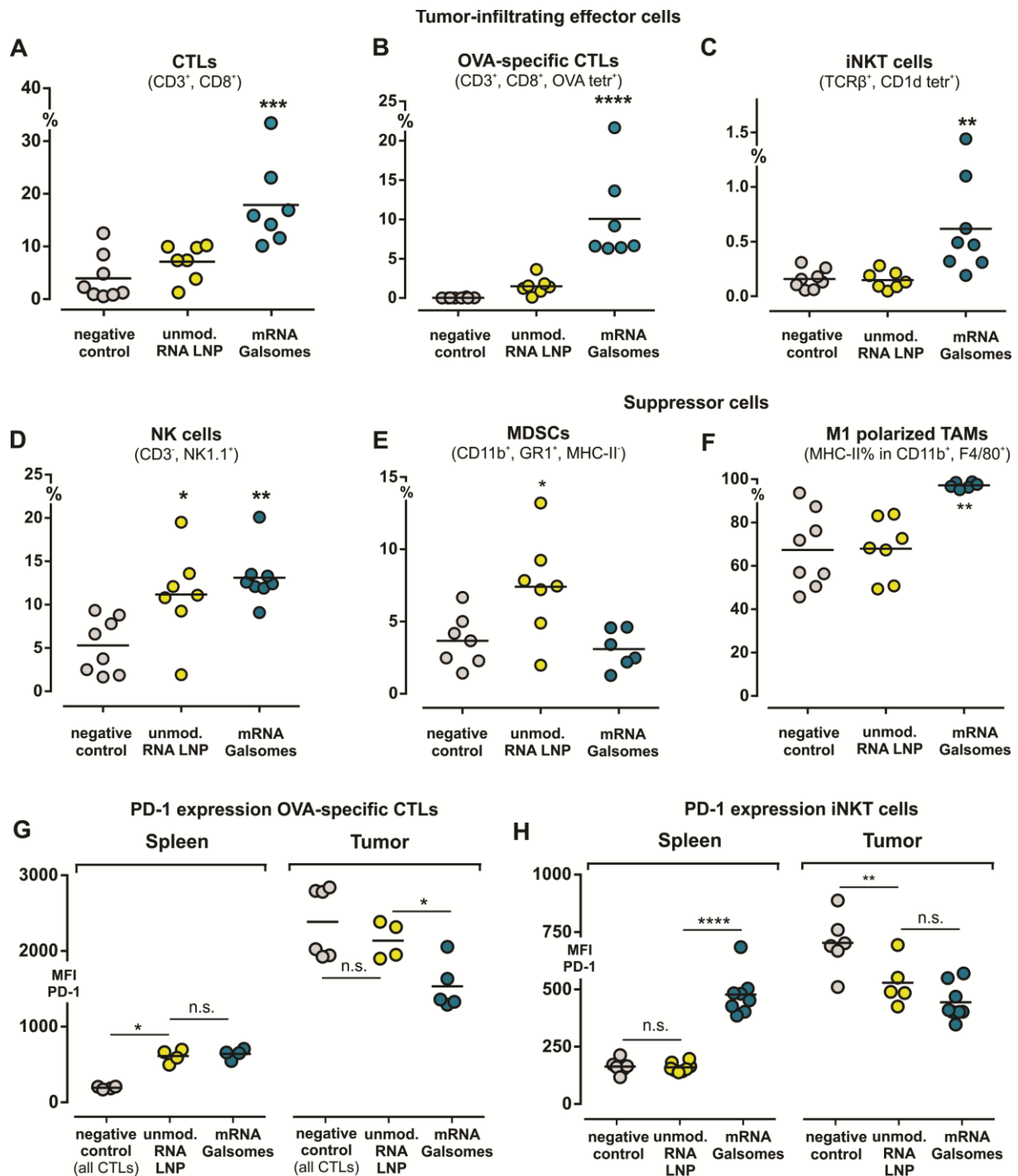
20 While vaccination with mRNA Galsomes resulted in “hot” T cell-infiltrated tumors, we  
21 investigated whether immune suppression *via* the PD-1/PD-L1 axis could be involved in  
22 countering the vaccine-induced immune response.<sup>29</sup> As shown in **Figure 5G**, LNP  
23 vaccination caused a significant up-regulation of PD-1 on the activated OVA-specific splenic  
24 CTLs compared to CTLs of untreated mice. These increased PD-1 levels were comparable for  
25 mice injected with mRNA Galsomes or LNPs containing unmodified mRNA. Within the

1 tumor, PD-1 levels on intratumoral CTLs are up to 10 times higher compared to CTLs in the  
2 spleen for untreated animals. Although PD-1 expression levels on intratumoral CTLs are  
3 lower in vaccinated animals, it remains obvious that in this microenvironment, the influence  
4 of the PD-1/PD-L1 axis is much more pronounced compared to the spleen. A different  
5 situation is observed for iNKT cells. As shown in **Figure 5H**, mRNA Galsomes not only  
6 trigger the proliferation of splenic iNKT cells, but this coincides with a doubling in their PD-1  
7 expression levels. LNPs containing unmodified mRNA without  $\alpha$ -GC, did not have this  
8 effect. Within the tumor, the crosstalk between iNKT cells and the tumor microenvironment  
9 once more results in stronger PD-1 expression in all treatment groups. This PD-1 up-  
10 regulation on previously activated iNKT cells matches previous reports where inhibitory  
11 signals *via* the PD-1/PDL-1 pathway were suggested to play a role in the loss of  
12 responsiveness to subsequent  $\alpha$ -GC stimulations after (over-) stimulation. Moreover, this is in  
13 line with the limited boost-effect we observed upon multiple injections of the mRNA  
14 Galsomes (**Figure 4C-D**).

15 In addition to expression levels of PD-1, we measured the presence of its ligand on DCs (in  
16 spleen and tumor), as well as on tumor cells, specifically for mRNA Galsomes  
17 (**Supplementary Figure S9**). Similar to other reports, we observed that  $37.5 \pm 4.9$  % of  
18 splenic DCs up-regulated the expression of PD-L1 after vaccination with mRNA Galsomes.  
19 Similar to what we observed for intratumoral PD-1 levels, DCs within the tumor exhibit much  
20 higher basal levels of PD-L1, which are further increased upon mRNA Galsome vaccination.  
21 When evaluating the tumor cells' PD-L1 levels, a fourfold increase in expression could be  
22 observed in animals treated with mRNA Galsomes compared to untreated controls.

23 Taken together, these findings demonstrate that the inhibitory PD-1/PD-L1 immune  
24 checkpoint axis is involved in the suppression of CTLs, and that it could potentially explain

1 the limited responsiveness of iNKT cells to a second (boost) vaccination, thus limiting  
 2 antitumor immunity.



3  
 4 **Figure 5.** Therapeutic vaccination with mRNA Galsomes attracts immune effector cells to the  
 5 tumor and positively affects suppressive myeloid cells in B16-OVA melanoma. B16-OVA  
 6 bearing mice which received two vaccinations with OVA mRNA Galsomes were euthanized

1 on day 14 and evaluated for infiltration CD8<sup>+</sup> T cells **(A)** and OVA-specific CD8<sup>+</sup> T cells **(B)**,  
2 iNKT cells **(C)** and NK cells **(D)**. **(E)** Presence of MDSCs (CD11b<sup>+</sup>, GR1<sup>+</sup>, MHC-II<sup>-</sup>) and **(F)**  
3 M1 polarized TAMs (CD11b<sup>+</sup>, F4/80<sup>+</sup>, MHC-II<sup>+</sup>) in tumor site ( $n=8$ , pooled from two  
4 independent experiments). **(G)** PD-1 expression on splenic and tumor-infiltrating OVA-  
5 specific CD8<sup>+</sup> T cells at day 14 (two days after boost) ( $n=4-6$ ). **(H)** PD-1 expression levels on  
6 (activated) iNKT cells in spleen and B16-OVA tumors at day 14 ( $n=5-8$ , pooled from two  
7 independent experiments). Statistical analyses on datasets were performed by One-Way  
8 ANOVA followed by Turkey's post hoc test. Asterisks indicate statistical significance  
9 compared to the untreated group (\*,  $p < 0.05$ ; \*\*,  $p < 0.01$ ; \*\*\*,  $p < 0.001$ ; \*\*\*\*,  $p < 0.0001$ ).

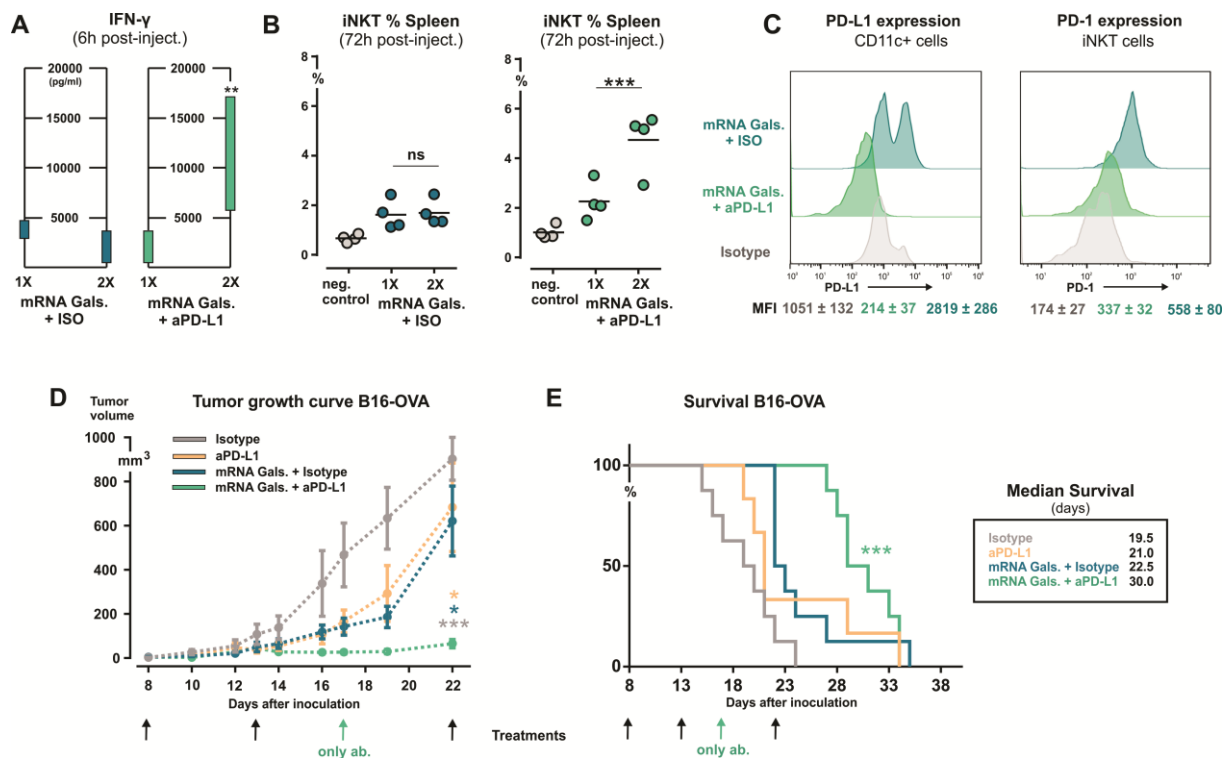
## 10 **Anti-PD-L1 checkpoint blockade synergizes with the antitumor effects of mRNA** 11 **Galsomes**

12 To first investigate the problem of iNKT anergy in more detail, naive mice were vaccinated  
13 twice with mRNA Galsomes with a five day interval. At respectively 6h and three days after  
14 each administration, we evaluated the cytokine release and iNKT activation. As shown in  
15 **Figure 6A**, IFN- $\gamma$  levels measured after the second vaccination, were only half of the levels  
16 measured after the first administration. In addition, we could observe a shift towards the  
17 production of IL-4 and IL-10, which counteract Th1 and therefore CTL responses  
18 **(Supplementary Figure S10)**. Finally, we noticed that a boost-vaccination with mRNA  
19 Galsomes did not further augment iNKT cell numbers, confirming the induction of a hypo-  
20 responsive state of iNKT cells. In shear contrast, when mice were simultaneously vaccinated  
21 and injected with an anti-PD-L1 antibody, IFN- $\gamma$  production rose up to four times higher after  
22 the second vaccination, compared to that after the initial challenge. Along the same line, the  
23 combination with an anti-PD-L1 antibody further boosted the expansion of iNKT cells, as a  
24 second administration doubled the number of splenic iNKT cells ( $2.25 \pm 0.7$  versus  $4.73 \pm 1.2$   
25 %, **Figure 6B**). Evaluation of PD-L1 on splenic DCs showed that the previously observed up-

1 regulation of this molecule upon mRNA Galsome vaccination could be fully eliminated by the  
2 concomitant delivery of an anti-PD-L1 antibody (**Figure 6E**).<sup>42, 43</sup> In addition, these data  
3 show that repeated activation of iNKT cells by the mRNA Galsomes/checkpoint combination  
4 strategy is feasible, as the PD-1 levels on iNKT cells were halved compared to levels in mice  
5 that merely received a single vaccination with mRNA Galsomes alone (**Figure 6C**).

6 To evaluate if the above-mentioned effects of the combination therapy could also be  
7 translated into an improved therapeutic outcome, B16-OVA bearing mice were vaccinated  
8 with mRNA Galsomes combined with intraperitoneal (i.p.) administrations of either an anti-  
9 PD-L1 antibody or an isotype control antibody. Monotherapy of an anti-PD-L1 or isotype  
10 control antibody was used as additional controls. The results in **Figure 6D** show that by the  
11 time of the last vaccination (day 22), the average tumor volume of mice treated with a  
12 combination of mRNA Galsome and a checkpoint blocking antibody, remained limited to  $59$   
13  $\pm 46$  mm<sup>3</sup>. By contrast, in all other groups, tumors had already grown up to 10 times larger.  
14 This also translated into a significant increase in median survival. Mice receiving  
15 monotherapy of an anti-PD-L1 antibody or mRNA Galsomes had reached their median  
16 survival at day 21 and 22.5, respectively, which is not significantly later than animals in the  
17 control group where only an isotype control antibody was injected (median survival of 19  
18 days). The combination treatment significantly prolonged median survival to 30 days,  
19 indicating a synergistic effect between both treatment strategies.

20 Overall, we clearly show that the therapeutic potential of mRNA Galsomes can be  
21 strengthened by rationally combining with PD-L1 checkpoint inhibition. This checkpoint  
22 blockage (1) prevents the induction of iNKT anergy allowing multiple vaccination rounds,  
23 and (2) avoids adaptive resistance mechanisms at the tumor site prolonging antitumor effects  
24 and promoting the survival of B16-OVA tumor-bearing mice.



1

2 **Figure 6.** Checkpoint inhibition with an anti-PD-L1 antibody prevents the induction of iNKT

3 energy and avoids adaptive resistance to antitumor effects of mRNA Galsomes. For the

4 evaluation of iNKT energy, naive mice received two subsequent injections with OVA mRNA

5 Galsomes at a five day interval. **(A)** Graph showing IFN- $\gamma$  levels in serum, collected 6h after

6 the first and second administration of mRNA Galsomes combined with either isotype or anti-

7 PD-L1 antibody. ( $n=4$ ). **(B)** Percentages of iNKT cells (TCR $\beta^+$ , mCD1d PBS-57 $^+$  cells)

8 among splenocytes, measured three days after each vaccination. **(C)** PD-L1 expression on

9 splenic DCs (CD11c $^+$  cells) and PD-1 expression on proliferated iNKT cells, measured 6h

10 after the first and three days after the second post vaccination, respectively ( $n=3-4$ ). B16-OVA

11 bearing mice were i.p. administered with 100  $\mu$ g of a rat IgG2b antibody (isotype control) or

12 anti-PD-L1 antibody in monotherapy, or in combination therapy with mRNA Galsomes.

13 Graph **(D)** shows average tumor growth curves and **(E)** Kaplan–Meier survival curves for

14 respective treatments, demonstrating synergistic effects between the anti-PD-L1 antibody and

15 mRNA Galsomes ( $n=6-8$ ). Black arrows indicate the days of treatment with both i.v. mRNA

1 Galsomes and i.p. antibody. Blue arrows indicate when only antibody was injected (i.p.).  
2 Pairwise statistical analysis in (A) and (B) were performed using a student's t test. For (D),  
3 tumor volumes at day 22 after tumor inoculation were compared by a One-way ANOVA  
4 followed by Tukey's post hoc test. Asterisks indicate statistical significance compared to the  
5 untreated group (n.s.,  $p > 0.05$ ; \*  $p < 0.05$ ; \*\*  $p < 0.01$ ; \*\*\*,  $p < 0.001$ ).

6

## 7 DISCUSSION

8 In this study, we report on the use of an mRNA nanovaccine that is capable of inducing a  
9 broad set of antitumor effector cells, including CTLs, iNKT cells and NK cells, while  
10 reducing local immune suppression at the tumor site. This was achieved by co-packaging  
11 nucleoside-modified mRNA encoding tumor antigens and the glycolipid  $\alpha$ -GC, which  
12 functions as an iNKT cell agonist and broadly acting immune adjuvant.

13 In the specific case of cancer immunotherapy, it was proven essential to evoke a systemic  
14 immune response to obtain antitumor immunity, which makes i.v. delivery the preferred  
15 administration route for mRNA-based cancer vaccines.<sup>5, 7, 44</sup> In our previous research, we  
16 showed that DOTAP-cholesterol nanoparticles could efficiently deliver mRNA to DCs and  
17 macrophages in lungs and spleen after systemic delivery.<sup>31</sup> By introducing modified  
18 nucleotides in the mRNA construct, the stability and translation are enhanced, resulting in  
19 higher and more sustainable mRNA expression levels. This enhanced mRNA expression is  
20 advantageous in the development of vaccines, since the resulting increased antigen  
21 presentation is shown to be beneficial for the induction of long-lived antibody and helper T  
22 cell responses, including the formation of follicular T cells.<sup>45</sup> However, nucleoside-modified  
23 mRNA largely loses its self-adjuvancy, resulting in reduced type I IFN levels, and a limited



1 capacity to evoke CTL immunity. To compensate for this, vaccines based on immunosilent  
2 mRNA require additional immune stimulation, which we provided by including  $\alpha$ -GC.<sup>6,31</sup>  
3 We demonstrated that by embedding the glycolipid  $\alpha$ -GC within mRNA DOTAP-cholesterol  
4 nanoparticles, the delivery of  $\alpha$ -GC and its subsequent CD1d-mediated presentation were  
5 enhanced, while the mRNA transfection remained equally high (**Figure 1**). In all likelihood,  
6 this can be attributed to a difference in cellular uptake, which largely determines the  
7 trafficking and loading into CD1d. Exogenous glycolipid antigens, can either directly  
8 associate with cell surface-bound CD1d or, when these lipids are present in the  
9 endolysosomal compartments, they can be complexed with CD1d, which is being recycled  
10 from the plasma membrane through the endosomes and lysosomes.<sup>46</sup> Especially this last form  
11 of  $\alpha$ -GC-CD1d complexation is interesting, as Torreno-Pina demonstrated that this process  
12 results in the formation of nanoclusters of CD1d-loaded  $\alpha$ -GC at the APC's surface, a process  
13 referred to as "lipid-raft mediated CD1d presentation".<sup>47</sup> Since the occurrence of larger  
14 nanoclusters is correlated with enhanced iNKT cell stimulation, superior DC licensing and  
15 improved transactivation of bystander NK cells, this pathway will likely proved the strongest  
16 immune adjuvant effect.<sup>48, 49</sup> Taken together, it is likely that by particulating  $\alpha$ -GC, it is  
17 preferentially trafficked through the endolysosomes, not only enabling a higher intracellular  
18 presence, but also resulting in superior lipid antigen presentation.

19 As a result of this enhanced  $\alpha$ -GC presentation capacity, mRNA Galsomes containing low  
20 doses of  $\alpha$ -GC were able to trigger the stimulation of iNKT cells *in vivo*, which rapidly  
21 induced the maturation of transfected APCs and coincided with the release of a plethora of  
22 cytokines (**Figure 2**). Shortly after the systemic delivery of mRNA Galsomes, we detected  
23 high levels of the Th1 cytokines IFN- $\gamma$ , TNF- $\alpha$  and IL-12p70, as well as of the Th2 cytokines  
24 IL-6 and IL-4. Similar to type I IFN, IL-12p70 acts as a "third signal cytokine", promoting the  
25 activation and survival of T cells<sup>50</sup>. We also detected high levels of IL-27, a stimulatory

1 cytokine that plays a pivotal role in the expansion and programming of T cells, and is  
2 involved in the regulation of NK and iNKT cells and their recruitment to the tumor site.<sup>51-53</sup> In  
3 connection herewith, Semmling *et al.* demonstrated that DCs licensed by iNKT cells recruited  
4 CTLs *via* a particular chemokine mechanism, comprising the production of CCL17 and the  
5 expression of CCR4.<sup>54, 55</sup> They showed that CCL17 acted synergistically with other  
6 chemokine pathways, resulting in more rapid and improved CTL responses. Indeed, we  
7 showed that vaccination with mRNA Galsomes resulted in approximately five times more  
8 antigen-specific CTLs compared to LNPs loaded with unmodified mRNA (**Figure 3**).

9 With respect to the therapeutic effects of mRNA Galsomes, we could determine a switch from  
10 a tumor-promoting towards a more antitumoral immune infiltrate within the tumor. First of  
11 all, we observed significantly higher levels of CTL, iNKT and NK cell levels after  
12 vaccination with mRNA Galsomes, compared to vaccination with gold standard particles  
13 containing unmodified mRNA (**Figure 3**). In this regard, it is important to consider that even  
14 without specifically targeting NK and iNKT cells in the vaccine design, it is known that these  
15 cells contribute to the outcome of therapeutic vaccines. As such, Fotin-Mleczek *et al.* showed  
16 that depletion of NK and iNKT cells *via* NK1.1 antibodies, partially reduced the antitumor  
17 effects of an mRNA vaccine encoding OVA in E.G7-OVA lymphoma implanted mice.<sup>56</sup>  
18 Therefore, the specific stimulation of iNKT responses by including glycolipid antigens can be  
19 expected to enhance the vaccine effect. Indeed, we observed a more favorable, antitumoral  
20 immune infiltrate in B16-OVA tumors treated with mRNA Galsomes compared to  
21 nanoparticles containing unmodified mRNA (**Figure 5**). mRNA Galsomes evoked a stronger  
22 infiltration of effector immune cells, with seven times more OVA-specific CTLs and  
23 approximately four times more iNKT cells. For NK cells, we found that the cell numbers in  
24 mRNA Galsomes-treated tumors had more than doubled compared to untreated controls,  
25 which matched levels evoked by vaccination with unmodified mRNA.

1 A second observation was the reduced presence of immunosuppressive tumor-infiltrating cells  
2 (Figure 5). To exemplify, mRNA Galsomes positively modulated suppressive myeloid cells in  
3 B16-OVA tumors, as demonstrated by the reduced infiltration of MDSCs and TAMs and their  
4 increased expression levels of MHC-II. These observations can be further explained by the  
5 research of Cortesi *et al.*, who evidenced that iNKT cells could, *via* CD1d and CD40/Fas-  
6 dependent cell interactions, selectively kill M2-like macrophages, while promoting the  
7 survival of M1-like macrophages.<sup>37</sup> Moreover, it was shown that iNKTs can mediate the  
8 conversion of immunosuppressive MDSCs into immunogenic APCs in a CD1d-dependent  
9 manner.<sup>36</sup> In addition, multiple studies provided evidence that the cytokine responses to  $\alpha$ -GC  
10 have the capacity to restore the functionality of tumor-suppressed DCs and exhausted CTLs,  
11 breaking local tolerance in the tumor microenvironment.<sup>53, 57</sup>

12 Despite these promising changes in the tumor immune infiltrate, mRNA Galsomes merely had  
13 a limited impact on tumor progression and survival of B16-OVA-bearing mice, which was  
14 comparable to the effects of gold-standard nanoparticles containing unmodified mRNA  
15 (**Figure 4**). In part, this could be linked to the observation that repeated vaccinations with  
16 mRNA Galsomes did not exert a boost effect on tumor reduction, nor did it evoke further  
17 expansion of iNKT cells. This strongly suggested the induction of a hypo-responsive or  
18 anergic state, which was previously reported to occur after strong iNKT activation by  $\alpha$ -  
19 GC.<sup>58-60</sup> This anergy is generally characterized by the impaired production of Th1 cytokines  
20 and reduction in iNKT cell numbers upon re-stimulation. While literature contains conflicting  
21 data about iNKT anergy, multiple studies reported that the PD-1/PD-L1 checkpoint pathway  
22 plays a critical role in regulation of iNKT cell activity.<sup>42, 57, 61</sup> When investigating the  
23 involvement of this checkpoint axis in the present study, we confirmed the up-regulation of  
24 PD-1 in activated NKT cells, as well as its ligand PD-L1 in APCs in the systemic organs  
25 (**Figure 5** and **Figure S9**). We could also detect a pronounced PD-L1 expression in tumors of

1 nanoparticle-treated animals. This coincided with high PD-1 expression levels on OVA-  
2 specific tumor infiltrating CTLs, which was both the case for animals treated with mRNA  
3 Galsomes and LNPs containing unmodified mRNA. This is consistent with recent research by  
4 Sayour *et al.*, who reported that i.v. administered DOTAP LNPs containing unmodified  
5 mRNA increased the levels of PD-L1 on myeloid cells in the systemic organs and in the  
6 tumor micro-environment.<sup>62</sup>

7 The identification of PD-1/PD-L1-mediated adaptive resistance as one of the culprit  
8 mechanisms that hamper the antitumoral effects of T cells and iNKT cells, also offers an  
9 additional therapeutic point of engagement.<sup>62-64</sup> Consequently, we tested the combination of  
10 mRNA Galsomes with i.p. administration of an anti-PD-L1 antibody (**Figure 6**). Indeed, the  
11 combination therapy showed clear synergistic antitumor effects in every treated mouse, while  
12 mRNA Galsomes and the anti-PD-L1 antibody in monotherapy only exerted antitumor effects  
13 in a small portion of animals. Additionally, we could demonstrate that the administration of  
14 an anti-PD-L1 antibody at the same time as the mRNA Galsome vaccine, prevented the  
15 induction of iNKT anergy, and allowed to boost the stimulation of iNKT cells after successive  
16 administrations. These findings confirm previous observations made by Parekh *et al.*  
17 combining unformulated  $\alpha$ -GC with antibodies directed against PD-L1 and PD-L2.<sup>42</sup>  
18 Importantly, one should bear in mind that recent studies suggest that the up-regulation of PD-  
19 1 by iNKT cells is only a small part of a complex immune cascade, involving different  
20 signalling pathways.<sup>65-68</sup> For instance, some reports showed associations between Wnt/ $\beta$ -  
21 catenin signalling and the regulation of cytokine responses by iNKT cells. More specifically,  
22 Kling *et al.* showed that upon challenge with  $\alpha$ -GC,  $\beta$ -catenin activity rapidly suppresses the  
23 production of IFN- $\gamma$  by iNKT cells in liver, while IL-4 production is promoted.<sup>67</sup> In addition,  
24 Berga-Bolaños *et al.* demonstrated that  $\beta$ -catenin expression promotes the development of  
25 iNKT2 and iNKT17 subsets in the thymus, at the expense of iNKT1 cells, potentially

1 explaining the polarization towards the production of Th2-biased cytokines upon sequential  $\alpha$ -  
2 GC stimulations.<sup>68</sup> Taken together, it is likely that by also counteracting these other  
3 suppressive mechanisms, iNKT cell anergy and the resistance to the therapeutic effects of  
4 mRNA Galsomes, could be further tuned down.

5 Finally, it is important to consider that B16-OVA tumor cells are notorious for their low  
6 expression of CD1d, which makes them poor targets for direct killing by iNKT cells. The  
7 mode of action of the mRNA Galsomes in this model is therefore expected to be almost  
8 exclusively determined by the indirect effects of iNKT activation: (i) the licensing of DCs by  
9 iNKT cells, (ii) the promotion of CTL responses and NK cell responses, and (iii) the  
10 beneficial interactions between iNKT cells and suppressive myeloid cells in the tumor micro-  
11 environment.<sup>32-34</sup> Therefore, we would like to stress that it is likely that the true value of the  
12 mRNA Galsomes will probably lie in the treatment of tumors where direct iNKT cell-  
13 mediated killing effects can occur. For example, in most blood cancers, such as lymphomas,  
14 tumor cells express CD1d, which makes them vulnerable to direct killing effects of iNKT  
15 cells.<sup>69-71</sup> Also, renal cell carcinoma, colorectal carcinoma and some brain cancers (*e.g.*,  
16 malignant glioma and in some cases of medullablastoma) were shown to be CD1d positive,  
17 with iNKT cell infiltration being a marker of favorable outcome in patients.<sup>69</sup>

18

## 19 CONCLUSION

20 Taken together, we have developed a flexible and versatile mRNA nanoparticle platform that  
21 presents an attractive way of initiating tumor immunity by targeting and activating  
22 conventional T cells and iNKT cells directly *in vivo*. Importantly, by combining immune-  
23 silent mRNA with the iNKT ligand  $\alpha$ -GC in a single particle, a broad, yet safe, effective and  
24 controllable immune response can be evoked in different tumor models. In combination

1 therapy with PD-1/PD-L1 checkpoint inhibition, mRNA Galsomes hold potential to achieve  
2 effective antitumor immunity, this by preventing the induction of iNKT anergy, as well as by  
3 overcoming adaptive resistance at the tumor site.

4

## 5 EXPERIMENTAL

### 6 **Cell culture and mice**

7 Female C57BL/6 mice (6 weeks old) were purchased from Envigo (Gannat, France) and  
8 housed in an SPF facility. All animal experiments were conducted according to the  
9 regulations of the Belgian law and approved by the local Ethical Committee. Primary murine  
10 bone marrow-derived DC (BM-DC) cultures were generated as previously described.<sup>31</sup>  
11 Briefly, bone marrow was isolated from the femurs and tibiae and processed into a single cell  
12 suspension. After red blood cell lysis, cells were cultured in complete medium (RPMI  
13 containing 5% FetalClone™ I (HyClone™), 1% penicillin/streptomycin/L-glutamin (Gibco-  
14 Invitrogen),  $\beta$ -mercaptoethanol (5  $\mu$ M, Gibco-Invitrogen) and 40 ng ml<sup>-1</sup> GM-CSF  
15 (PeproTech) in low-adherence culture dishes. At day 5, all cells were collected by  
16 centrifugation, resuspended in the complete medium and seeded for experiments at 5x10<sup>5</sup>  
17 cells per well in a 24 well plate.

18 The mouse melanoma cell line B16-OVA (kindly provided by K. Rock, University of  
19 Massachusetts Medical Center) and the T cell lymphoma E.G7-OVA (obtained from the  
20 American Type Culture Collection, Rockville, MD, USA) were cultured at 37°C in a  
21 humidified 5% CO<sub>2</sub> atmosphere in RPMI 1640 medium (Sigma-Aldrich, Diegem, Belgium)  
22 supplemented with 10% FBS, 100 U ml<sup>-1</sup> penicillin, 100  $\mu$ g ml<sup>-1</sup> streptomycin, 2 mM l-  
23 glutamine and 0.4 mg ml<sup>-1</sup> of the selection agent G418 (Thermo-Scientific, Aalst, Belgium).

## 1 mRNA constructs

2 Unmodified and nucleoside-modified (5meC,  $\Psi$ ) mRNA encoding firefly luciferase (fLuc)  
3 and the enhanced green fluorescent protein (eGFP) were purchased from TriLink (San Diego,  
4 CA). For the immunization studies, a truncated form of ovalbumin (tOVA) fused to the first  
5 80 amino acids of the invariant chain (Ii80) was produced by *in vitro* mRNA transcription  
6 from pGEM-Ii80tOVA plasmids.<sup>72</sup> The *in vitro* transcription of mRNA and its subsequent  
7 quality control were performed as previously described.<sup>31</sup> For the transcription of nucleoside-  
8 modified mRNA, cytidine and uridine nucleotides were 100% replaced by 5-methylcytidine  
9 and pseudouridine (TriLink).

## 10 mRNA lipid nanoparticle preparation

11 DOTAP (1,2-dioleoyl-3-trimethylammonium-propane) and cholesterol were purchased from  
12 Avanti Polar Lipids (Alabaster, USA). Alpha-Galactosylceramide ( $\alpha$ -GC) and 6''-BODIPY-  
13 analogue of  $\alpha$ -GC were synthesized in house by S. Van Calenbergh. The synthesis of  $\alpha$ -GC  
14 was performed as previously described.<sup>73</sup> A detailed description of the preparation of  
15 BODIPY-labelled  $\alpha$ -GC can be found in **Supplementary Information**. Cationic liposomes of  
16 DOTAP-cholesterol (2:3 molar ratio) were prepared by transferring the appropriate amounts  
17 of lipids, dissolved in chloroform into a round-bottom flask. For liposomes formulated with  $\alpha$ -  
18 GC, 0.5, 0.15, 0.015 or 0.0015 mol% of the total lipid amount was replaced by  $\alpha$ -GC. The  
19 chloroform was evaporated under nitrogen, after which the lipid film was rehydrated in  
20 HEPES buffer (20 mM, pH 7.4, Sigma-Aldrich) to obtain a final lipid concentration of  
21 12.5 mM. The resulting cationic liposomes were sonicated until the dispersion became clear in  
22 a bath sonicator (Branson Ultrasonics, Dansbury, USA). Then, they were mixed with mRNA  
23 to obtain mRNA nanoparticles at a cationic lipid-to-mRNA (N/P) ratio of 3. mRNA

1 nanoparticles for *in vivo* use were prepared in an isotonic HEPES buffer containing 5%  
2 glucose (Sigma-Aldrich).

### 3 ***In vitro* evaluation of $\alpha$ -GC delivery and presentation by BM-DCs**

4 The *in vitro* experiments were performed on BM-DCs at day 6 of cell culture. The day before  
5 transfection, cells were seeded in 24 well plates at  $5 \times 10^5$  cells per well, and grown in the cell  
6 culture medium with 5% FCI serum. mRNA nanoparticles containing 0.5 mol% of  $\alpha$ -GC were  
7 added directly to the cells in the complete cell culture medium (1  $\mu$ g mRNA per  $5 \times 10^5$  cells).  
8 As a control, an equimolar dose of  $\alpha$ -GC alone was added, dissolved in DMSO. To evaluate  
9 the presentation of  $\alpha$ -GC in cell-surface CD1d complexes, BM-DCs cells were surface-stained  
10 with a monoclonal antibody specific for  $\alpha$ -GC-CD1d complexes (clone L363, eBioscience).  
11 Flow analysis was performed 24h after the addition of mRNA nanoparticles (fLuc mRNA).  
12 Cells were collected and washed with PBS, stained with a fixable viability dye eFluor<sup>®</sup> 450  
13 (eBioscience) according to the manufacturer's instructions, incubated with Fc block  
14 (CD16/32) to block non-specific FcR binding (BD Biosciences, Erembodegem, Belgium), and  
15 surface stained for CD11c-APC (clone N418) and  $\alpha$ -GC:CD1d complex-PE for 30 min at  
16 4°C. Mouse IgG2a kappa PE antibody was used as isotype control for the presentation of  $\alpha$ -  
17 GC:CD1d. After additional washing steps, the cells were analysed by flow cytometry using a  
18 CytoFLEX (Beckman Coulter, Krefeld, Germany) and analysis was performed using FlowJo  
19 software (FlowJo, OR, USA). Confocal microscopy images of the cells were recorded using a  
20 Nikon C1si confocal laser scanning module attached to a motorized Nikon TE2000-E inverted  
21 microscope (Nikon Benelux, Brussels, Belgium), equipped with a Plan Apo 60x 1.0 NA oil  
22 immersion objective lens (Nikon).

### 23 **Administration of mRNA nanoparticles and an anti-PD-L1 antibody**



1 Mice were anesthetized in a ventilated anesthesia chamber with 3% isoflurane in oxygen.  
2 Prior to injection, a catheter of polyethylene tubing (Intramedic PE10, BD) containing sterile  
3 0.9% NaCl solution was inserted in the tail vein. After correct placement, nanoparticles with  
4 the indicated cargo diluted in sterile 5% glucose HEPES buffer were slowly injected (200  $\mu$ l).  
5 A dose of 10  $\mu$ g mRNA per mouse was chosen based on previous mRNA dose-optimization  
6 studies. The optimized dose of nanoparticle-encapsulated  $\alpha$ -GC was 20 ng per mouse (0.015  
7 mol%), determined based on cytokine production and iNKT activation. Anti-PD-L1 antibody  
8 (10F.9G2, Bio X cell, West Lebanon, USA) or rat IgG2b isotype control antibody (LTF-2,  
9 Bio X cell) was administered i.p. at a dose of 100  $\mu$ g, immediately after the administration of  
10 mRNA nanoparticles.

### 11 **Bioluminescence imaging**

12 Six hours after the injection of nanoparticles containing fLuc mRNA (TriLink), mice were  
13 anesthetized and abdomen and chest were depilated with hair removal cream. Subsequently,  
14 VivoGlo™ Luciferin (Promega) was administered i.p. in a volume of 100  $\mu$ l (33 mg ml<sup>-1</sup>) per  
15 mouse. After 10 min, bioluminescence images were acquired by the IVIS lumina II system  
16 (PerkinElmer, Waltham, MA), and quantitative analysis of the images was performed using  
17 the Living Image software (PerkinElmer).

### 18 **Therapeutic vaccination experiments**

19 The therapeutic potential of mRNA nanoparticles (containing different cargo, or in  
20 combination with an anti-PD-L1 antibody) was evaluated by performing therapeutic  
21 vaccinations in tumor-bearing mice. For this, C57BL/6 received a s.c. injection of  $3 \times 10^5$  B16-  
22 OVA or E.G7-OVA tumor cells (suspended in PBS) in the flank. Eight days after tumor  
23 inoculation, when the lesions were palpable, the mice were randomized in different treatment  
24 groups based on tumor volume, and vaccinated with mRNA nanoparticles. In some

1 experiments, animals received a second and third therapeutic vaccination, every four or five  
2 days. Tumor growth was measured every other day or two days using a digital caliper. When  
3 the tumor volume exceeded 1000 mm<sup>3</sup> (B16-OVA) or 1500 mm<sup>3</sup> (E.G7-OVA), the mice were  
4 euthanized *via* cervical dislocation.

### 5 **Flow cytometric analysis on single cell suspensions**

6 At different time points after immunization, mice were euthanized and spleen, lungs, liver and  
7 tumors were harvested and processed into single cell suspensions as previously described.<sup>31</sup>  
8 Single cell suspensions were stained with either a fixable viability dye eFluor<sup>®</sup> 450 (Thermo  
9 Scientific) or Zombie Yellow<sup>™</sup> (Biolegend, San Diego, CA) according to the manufacturer's  
10 instructions to exclude dead cells from analysis, incubated with Fc block (CD16/32) to block  
11 non-specific FcR binding (BD Biosciences, Erembodegem, Belgium), and surface stained  
12 with the indicated antibodies during 30 min at 4°C (all Thermo-Scientific). After additional  
13 washing steps, the cells were analyzed by flow cytometry. Compensation for spectral overlap  
14 was calculated using UltraComp eBeads<sup>™</sup> Compensation Beads (Thermo-Scientific) stained  
15 with individual fluorochrome-conjugated antibodies.

16 The activation state of DC positive for CD11c-(APC or FITC) in the spleen was analysed by  
17 measuring the up-regulation of the co-stimulatory molecules CD40-FITC (HM40-3), CD86-  
18 FITC (CL1), CD80-PE/Cy7 (16-10A1), and the inhibitory molecule PD-L1-Super Bright 436  
19 (MIH5). T cells were stained with monoclonal antibodies, including CD3e-PE (145-2C11),  
20 CD4-FITC (GK1.5), CD8a-(APC or AF488) (53-6.7) and PD-1-(eFl450 or FITC) (RMP1-30).  
21 To stain OVA-specific T cells, an BV450-conjugated H-2Kb/SIINFEKL tetramer (OVA-  
22 tetramer) was used, obtained from the National Institutes of Health (NIH) Tetramer Core  
23 Facility. iNKT cells were stained with TCRβ-APC (H57-597), PD1-eFl450 and mCD1d PBS-  
24 57 PE tetramer obtained from the NIH tetramer Core Facility. NK cells were detected using

1 CD3e-PE (negative gating) and NK1.1-APC (PK136) staining. In addition, myeloid derived  
2 suppressor cells (MDSCs) and tumor-associated macrophages (TAMs) were stained with  
3 antibodies including, CD11b-PE/Dazzle™ 594 (Biolegend), MHC-II-efl450 (M5/114.15.2),  
4 F4/80-(FITC or AF700) (6F12), Ly-6G/Ly-6C-FITC (RB6-8C5) and CD206-APC (C068C2).  
5 DCs (CD11c<sup>+</sup>) and tumor cells (CD45-PerCP-Cy5.5 negative cells) were evaluated for the  
6 expression of PD-L1.

### 7 **Cytokine measurements and alanine transaminase (ALT) activity**

8 Serum was collected 6h after i.v. injection of the mRNA nanoparticles and samples were  
9 stored at -80°C. Mouse Platinum IFN alpha ELISA kit , IFN- $\gamma$  and IL-4 ELISA kits (Ready-  
10 SET-Go!<sup>®</sup>) were purchased from Thermo-Scientific. A panel of 13 other cytokines, including  
11 IL-1 $\alpha$ , IL-1 $\beta$ , IL-6, IL-10, IL-12p70, IL-17A, IL-23, IL-27, MCP-1, IFN- $\beta$ , IFN- $\gamma$ , TNF- $\alpha$ ,  
12 and GM-CSF, was quantified using a multiplex assay (LEGENDplex™ Mouse Inflammation  
13 Panel, Biolegend). ALT enzyme activity was measured using a colometric assay kit  
14 (MaxDiscovery™, Bioo Scientific Corporation, Austin, USA). All assays were performed  
15 according to the manufacturer's instructions.

### 16 **Statistical analysis**

17 All data are presented as mean  $\pm$  standard deviation. Presented data of the *in vitro*  
18 experiments are representative for at least 3 independent experiments performed on three  
19 different days. The *in vivo* experiments contain data of at least two experiments merged into a  
20 single graph, this is explicitly mentioned in the figure caption. All statistical analysis were  
21 performed using GraphPad Prism6 (La Jolla, CA, USA). Information on the analysis per  
22 (sub)figure, is specified in the figure caption.

23 ASSOCIATED CONTENT

## 1 **Supporting Information.**

2 The following files are available free of charge. Supplementary figures showing the uptake of  
3 BODIPY-a-GC by BM-DCs, when formulated in mRNA Galsomes or dissolved in DMSO,  
4 the transfection capacity of mRNA Galsomes in BM-DCs and human monocyted-derived  
5 DCs, the adjuvant effect of mRNA Galsomes on BM-DCs *in vitro*, the toxicity evaluation of  
6 mRNA Galsomes in monotherapy and combined with an anti-PD-L1 antibody, the tumor  
7 growth in established E.G7-OVA tumors after vaccination with nanoparticles packaging  
8 nucleoside-modified mRNA alone, the comparison between one or two administrations of  
9 mRNA Galsomes to achieve antitumor immunity in E.G7-OVA bearing mice, the flow  
10 cytometric analysis of the immune filtrate of isolated tumors, the PD-L1 expression on splenic  
11 DCs, intratumoral DCs, and tumor cells after vaccination with mRNA Galsomes, the  
12 comparison between the cytokine responses after a first and second exposure to mRNA  
13 Galsomes (PDF).

## 14 **AUTHOR INFORMATION**

### 15 **Corresponding Author**

16 \* Corresponding author at: Ghent Research Group on Nanomedicines, Ottergemsesteenweg  
17 460, 9000 Ghent, Belgium. Tel.: +32 9 264 80 78; fax: +32 9 264 81 89. E-mail address:  
18 Stefaan.DeSmedt@UGent.be (S.C. De Smedt).

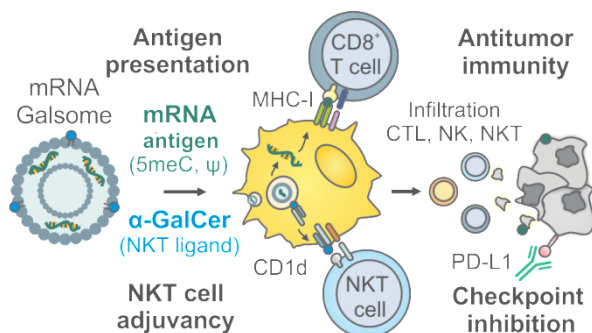
19 **Author contributions:** Designing research studies: R.V., H.D, I.L., and S.C.D. Conducting  
20 experiments: R.V. and H.D. Providing reagents: S.C.D, K.B, and S.V. Writing the  
21 manuscript: R.V, H.D, I.L and S.C.D. ‡ Last authors S.C.D and H.D. contributed equally to  
22 this work.

23

1 ACKNOWLEDGMENT

2 The authors would like thank E. Thuy Linh Achten for her help with the experimental work,  
3 L. Pieters and H. Declercq for the sample preparation for the histopathology study, and M.  
4 Van Bockstal for the histopathological analysis. They further wish to thank the NIH Tetramer  
5 Core Facility for providing H-2Kb/SIINFEKL tetramer and mCD1d PBS-57 tetramers. H.  
6 Dewitte is a postdoctoral fellow of the Research Foundation-Flanders, Belgium (FWO-  
7 Vlaanderen; grant No. 12E3916N). This research is supported by the FWO grants No.  
8 G016513N and G0B2814N and the Flemish agency for Innovation trough Science and  
9 Technology (IWT SBO NanoComit). Competing interests: Patent filed (application no.  
10 EP18195181.5, Therapeutic nanoparticles and methods of use thereof).

11 GRAPHICAL TABLE OF CONTENTS



13 REFERENCES

14 1. Sahin, U.; Kariko, K.; Tureci, O., mRNA-Based Therapeutics--Developing a New  
15 Class of Drugs. *Nat. Rev. Drug Discovery* **2014**, *13*, 759-780.  
16 2. Sayour, E. J.; De Leon, G.; Pham, C.; Grippin, A.; Kemeny, H.; Chua, J.; Huang, J.;  
17 Sampson, J. H.; Sanchez-Perez, L.; Flores, C.; Mitchell, D. A., Systemic Activation of  
18 Antigen-Presenting Cells via RNA-Loaded Nanoparticles. *Oncoimmunology* **2017**, *6*,  
19 e1256527.  
20 3. Abraham, M. K.; Peter, K.; Michel, T.; Wendel, H. P.; Krajewski, S.; Wang, X.,  
21 Nanoliposomes for Safe and Efficient Therapeutic mRNA Delivery: A Step toward  
22 Nanotheranostics in Inflammatory and Cardiovascular Diseases as Well as Cancer.  
23 *Nanotheranostics* **2017**, *1*, 154-165.  
24 4. Phua, K. K.; Staats, H. F.; Leong, K. W.; Nair, S. K., Intranasal mRNA Nanoparticle  
25 Vaccination Induces Prophylactic and Therapeutic Anti-Tumor Immunity. *Sci. Rep.* **2014**, *4*,  
26 5128.

- 1 5. Kranz, L. M.; Diken, M.; Haas, H.; Kreiter, S.; Loquai, C.; Reuter, K. C.; Meng, M.;  
2 Fritz, D.; Vascotto, F.; Hefesha, H.; Grunwitz, C.; Vormehr, M.; Husemann, Y.; Selmi, A.;  
3 Kuhn, A. N.; Buck, J.; Derhovanessian, E.; Rae, R.; Attig, S.; Diekmann, J. *et al.*, Systemic  
4 RNA Delivery to Dendritic Cells Exploits Antiviral Defence for Cancer Immunotherapy.  
5 *Nature* **2016**, *534*, 396-401.
- 6 6. Oberli, M. A.; Reichmuth, A. M.; Dorkin, J. R.; Mitchell, M. J.; Fenton, O. S.;  
7 Jaklenec, A.; Anderson, D. G.; Langer, R.; Blankschtein, D., Lipid Nanoparticle Assisted  
8 mRNA Delivery for Potent Cancer Immunotherapy. *Nano Lett.* **2017**, *17*, 1326-1335.
- 9 7. Broos, K.; Van der Jeught, K.; Puttemans, J.; Goyvaerts, C.; Heirman, C.; Dewitte, H.;  
10 Verbeke, R.; Lentacker, I.; Thielemans, K.; Breckpot, K., Particle-Mediated Intravenous  
11 Delivery of Antigen mRNA Results in Strong Antigen-Specific T-Cell Responses Despite the  
12 Induction of Type I Interferon. *Mol. Ther. Nucleic Acids* **2016**, *5*, e326.
- 13 8. Liu, L.; Wang, Y.; Miao, L.; Liu, Q.; Musetti, S.; Li, J.; Huang, L., Combination  
14 Immunotherapy of MUC1 mRNA Nano-Vaccine and CTLA-4 Blockade Effectively Inhibits  
15 Growth of Triple Negative Breast Cancer. *Mol. Ther.* **2018**, *26*, 45-55.
- 16 9. Rosigkeit, S.; Meng, M.; Grunwitz, C.; Gomes, P.; Kreft, A.; Hayduk, N.; Heck, R.;  
17 Pickert, G.; Ziegler, K.; Abassi, Y.; Roder, J.; Kaps, L.; Vascotto, F.; Beissert, T.; Witzel, S.;  
18 Kuhn, A.; Diken, M.; Schuppan, D.; Sahin, U.; Haas, H. *et al.*, Monitoring Translation  
19 Activity of mRNA -Loaded Nanoparticles in Mice. *Mol. Pharmaceutics* **2018**, *15*, 3909-3919.
- 20 10. Anderson, B. R.; Muramatsu, H.; Nallagatla, S. R.; Bevilacqua, P. C.; Sansing, L. H.;  
21 Weissman, D.; Karikó, K., Incorporation of Pseudouridine into mRNA Enhances Translation  
22 by Diminishing PKR Activation. *Nucleic Acids Res.* **2010**, *38*, 5884-5892.
- 23 11. Andries, O.; Mc Cafferty, S.; De Smedt, S. C.; Weiss, R.; Sanders, N. N.; Kitada, T.,  
24 N(1)-Methylpseudouridine-Incorporated mRNA Outperforms Pseudouridine-Incorporated  
25 mRNA by Providing Enhanced Protein Expression and Reduced Immunogenicity in  
26 Mammalian Cell Lines and Mice. *J. Controlled Release* **2015**, *217*, 337-344.
- 27 12. Kariko, K.; Buckstein, M.; Ni, H.; Weissman, D., Suppression of RNA Recognition by  
28 Toll-Like Receptors: The Impact of Nucleoside Modification and the Evolutionary Origin of  
29 RNA. *Immunity* **2005**, *23*, 165-175.
- 30 13. Kariko, K.; Muramatsu, H.; Welsh, F. A.; Ludwig, J.; Kato, H.; Akira, S.; Weissman,  
31 D., Incorporation of Pseudouridine into mRNA Yields Superior Nonimmunogenic Vector  
32 with Increased Translational Capacity and Biological Stability. *Mol. Ther.* **2008**, *16*, 1833-  
33 1840.
- 34 14. Pardi, N.; Hogan, M. J.; Porter, F. W.; Weissman, D., mRNA Vaccines - a New Era in  
35 Vaccinology. *Nat. Rev. Drug Discovery* **2018**, *17*, 261-279.
- 36 15. Bahl, K.; Senn, J. J.; Yuzhakov, O.; Bulychev, A.; Brito, L. A.; Hassett, K. J.; Laska,  
37 M. E.; Smith, M.; Almarsson, O.; Thompson, J.; Ribeiro, A. M.; Watson, M.; Zaks, T.;  
38 Ciaramella, G., Preclinical and Clinical Demonstration of Immunogenicity by mRNA  
39 Vaccines against H10N8 and H7N9 Influenza Viruses. *Mol. Ther.* **2017**, *25*, 1316-1327
- 40 16. Alberer, M.; Gnad-Vogt, U.; Hong, H. S.; Mehr, K. T.; Backert, L.; Finak, G.;  
41 Gottardo, R.; Bica, M. A.; Garofano, A.; Koch, S. D.; Fotin-Mleczek, M.; Hoerr, I.; Clemens,  
42 R.; von Sonnenburg, F., Safety and Immunogenicity of a mRNA Rabies Vaccine in Healthy  
43 Adults: An Open-Label, Non-Randomised, Prospective, First-in-Human Phase 1 Clinical  
44 Trial. *Lancet* **2017**, *390*, 1511-1520.
- 45 17. Iavarone, C.; O'Hagan D, T.; Yu, D.; Delahaye, N. F.; Ulmer, J. B., Mechanism of  
46 Action of mRNA -Based Vaccines. *Expert Rev. Vaccines* **2017**, *16*, 871-881.
- 47 18. Liang, F.; Lindgren, G.; Lin, A.; Thompson, E. A.; Ols, S.; Rohss, J.; John, S.;  
48 Hassett, K.; Yuzhakov, O.; Bahl, K.; Brito, L. A.; Salter, H.; Ciaramella, G.; Lore, K.,  
49 Efficient Targeting and Activation of Antigen-Presenting Cells in Vivo after Modified mRNA  
50 Vaccine Administration in Rhesus Macaques. *Mol. Ther.* **2017**, *25*, 2635-2647.

- 1 19. Grabbe, S.; Haas, H.; Diken, M.; Kranz, L. M.; Langguth, P.; Sahin, U., Translating  
2 Nanoparticulate-Personalized Cancer Vaccines into Clinical Applications: Case Study with  
3 RNA-Lipoplexes for the Treatment of Melanoma. *Nanomedicine (London, U.K.)* **2016**, *11*,  
4 2723-2734.
- 5 20. Pepini, T.; Pulichino, A.-M.; Carsillo, T.; Carlson, A. L.; Sari-Sarraf, F.; Ramsauer,  
6 K.; Debasitis, J. C.; Maruggi, G.; Otten, G. R.; Geall, A. J.; Yu, D.; Ulmer, J. B.; Iavarone, C.,  
7 Induction of an IFN-Mediated Antiviral Response by a Self-Amplifying RNA Vaccine:  
8 Implications for Vaccine Design. *J. Immunol.* **2017**, *198*, 4012-4024.
- 9 21. De Beuckelaer, A.; Pollard, C.; Van Lint, S.; Roose, K.; Van Hoecke, L.; Naessens,  
10 T.; Udhayakumar, V. K.; Smet, M.; Sanders, N.; Lienenklaus, S.; Saelens, X.; Weiss, S.;  
11 Vanham, G.; Grooten, J.; De Koker, S., Type I Interferons Interfere with the Capacity of  
12 mRNA Lipoplex Vaccines to Elicit Cytolytic T Cell Responses. *Mol. Ther.* **2016**, *24*, 2012-  
13 2020.
- 14 22. Crouse, J.; Kalinke, U.; Oxenius, A., Regulation of Antiviral T Cell Responses by  
15 Type I Interferons. *Nat. Rev. Immunol.* **2015**, *15*, 231-242.
- 16 23. De Beuckelaer, A.; Grooten, J.; De Koker, S., Type I Interferons Modulate CD8+ T  
17 Cell Immunity to mRNA Vaccines. *Trends Mol. Med.* **2017**, *23*, 216-226.
- 18 24. Jonasch, E.; Haluska, F. G., Interferon in Oncological Practice: Review of Interferon  
19 Biology, Clinical Applications, and Toxicities. *Oncologist* **2001**, *6*, 34-55.
- 20 25. Theofilopoulos, A. N.; Baccala, R.; Beutler, B.; Kono, D. H., Type I Interferons  
21 (Alpha/Beta) in Immunity and Autoimmunity. *Annu. Rev. Immunol.* **2005**, *23*, 307-336.
- 22 26. Sharma, P.; Hu-Lieskovan, S.; Wargo, J. A.; Ribas, A., Primary, Adaptive, and  
23 Acquired Resistance to Cancer Immunotherapy. *Cell* **2017**, *168*, 707-723.
- 24 27. Garcia-Diaz, A.; Shin, D. S.; Moreno, B. H.; Saco, J.; Escuin-Ordinas, H.; Rodriguez,  
25 G. A.; Zaretsky, J. M.; Sun, L.; Hugo, W.; Wang, X.; Parisi, G.; Saus, C. P.; Torrejon, D. Y.;  
26 Graeber, T. G.; Comin-Anduix, B.; Hu-Lieskovan, S.; Damoiseaux, R.; Lo, R. S.; Ribas, A.,  
27 Interferon Receptor Signaling Pathways Regulating PD-L1 and PD-L2 Expression. *Cell Rep.*  
28 **2017**, *19*, 1189-1201.
- 29 28. Sun, C.; Mezzadra, R.; Schumacher, T. N., Regulation and Function of the PD-L1  
30 Checkpoint. *Immunity* **2018**, *48*, 434-452.
- 31 29. Juneja, V. R.; McGuire, K. A.; Manguso, R. T.; LaFleur, M. W.; Collins, N.; Haining,  
32 W. N.; Freeman, G. J.; Sharpe, A. H., PD-L1 on Tumor Cells Is Sufficient for Immune  
33 Evasion in Immunogenic Tumors and Inhibits CD8 T Cell Cytotoxicity. *J. Exp. Med.* **2017**,  
34 *214*, 895-904.
- 35 30. Anderson, K. G.; Stromnes, I. M.; Greenberg, P. D., Obstacles Posed by the Tumor  
36 Microenvironment to T Cell Activity: A Case for Synergistic Therapies. *Cancer Cell* **2017**,  
37 *31*, 311-325.
- 38 31. Verbeke, R.; Lentacker, I.; Wayteck, L.; Breckpot, K.; Van Bockstal, M.; Descamps,  
39 B.; Vanhove, C.; De Smedt, S. C.; Dewitte, H., Co-Delivery of Nucleoside-Modified mRNA  
40 and TLR Agonists for Cancer Immunotherapy: Restoring the Immunogenicity of  
41 Immunosilent mRNA. *J. Controlled Release* **2017**, *266*, 287-300.
- 42 32. Godfrey, D. I.; Le Nours, J.; Andrews, D. M.; Uldrich, A. P.; Rossjohn, J.,  
43 Unconventional T Cell Targets for Cancer Immunotherapy. *Immunity* **2018**, *48*, 453-473.
- 44 33. Bedard, M.; Salio, M.; Cerundolo, V., Harnessing the Power of Invariant Natural  
45 Killer T Cells in Cancer Immunotherapy. *Front. Immunol.* **2017**, *8*, 1829.
- 46 34. Krijgsman, D.; Hokland, M.; Kuppen, P. J. K., The Role of Natural Killer T Cells in  
47 Cancer-a Phenotypical and Functional Approach. *Front. Immunol.* **2018**, *9*, 367.
- 48 35. Fujii, S.; Shimizu, K.; Smith, C.; Bonifaz, L.; Steinman, R. M., Activation of Natural  
49 Killer T Cells by  $\alpha$ -Galactosylceramide Rapidly Induces the Full Maturation of Dendritic

1 Cells in Vivo and Thereby Acts as an Adjuvant for Combined CD4 and CD8 T Cell Immunity  
2 to a Coadministered Protein. *J. Exp. Med.* **2003**, *198*, 267-279.

3 36. Ko, H. J.; Lee, J. M.; Kim, Y. J.; Kim, Y. S.; Lee, K. A.; Kang, C. Y.,  
4 Immunosuppressive Myeloid-Derived Suppressor Cells Can Be Converted into Immunogenic  
5 APCs with the Help of Activated NKT Cells: An Alternative Cell-Based Antitumor Vaccine.  
6 *J. Immunol.* **2009**, *182*, 1818-1828.

7 37. Cortesi, F.; Delfanti, G.; Grilli, A.; Calcinotto, A.; Gorini, F.; Pucci, F.; Luciano, R.;  
8 Grioni, M.; Recchia, A.; Benigni, F.; Briganti, A.; Salonia, A.; De Palma, M.; Bicciato, S.;  
9 Doglioni, C.; Bellone, M.; Casorati, G.; Dellabona, P., Bimodal CD40/Fas-Dependent  
10 Crosstalk between iNKT Cells and Tumor-Associated Macrophages Impairs Prostate Cancer  
11 Progression. *Cell Rep.* **2018**, *22*, 3006-3020.

12 38. Riese, P.; Trittel, S.; May, T.; Cicin-Sain, L.; Chambers, B. J.; Guzman, C. A.,  
13 Activated NKT Cells Imprint NK-Cell Differentiation, Functionality and Education. *Eur. J.*  
14 *Immunol.* **2015**, *45*, 1794-1807.

15 39. Haraguchi, K.; Takahashi, T.; Nakahara, F.; Matsumoto, A.; Kurokawa, M.; Ogawa,  
16 S.; Oda, H.; Hirai, H.; Chiba, S., CD1d Expression Level in Tumor Cells Is an Important  
17 Determinant for Anti-Tumor Immunity by Natural Killer T Cells. *Leuk. Lymphoma* **2006**, *47*,  
18 2218-2223.

19 40. Diken, M.; Kreiter, S.; Selmi, A.; Britten, C. M.; Huber, C.; Tureci, O.; Sahin, U.,  
20 Selective Uptake of Naked Vaccine RNA by Dendritic Cells Is Driven by Macropinocytosis  
21 and Abrogated Upon DC Maturation. *Gene Ther.* **2011**, *18*, 702-708.

22 41. Devoldere, J.; Dewitte, H.; De Smedt, S. C.; Remaut, K., Evading Innate Immunity in  
23 Nonviral mRNA Delivery: Don't Shoot the Messenger. *Drug Discovery Today* **2015**, *21*, 11-  
24 25

25 42. Parekh, V. V.; Lalani, S.; Kim, S.; Halder, R.; Azuma, M.; Yagita, H.; Kumar, V.;  
26 Wu, L.; Van Kaer, L., PD-1:PD-L Blockade Prevents Anergy Induction and Enhances the  
27 Anti-Tumor Activities of Glycolipid-Activated iNKT Cells. *J. Immunol.* **2009**, *182*, 2816-  
28 2826.

29 43. Wang, J.; Cheng, L.; Wondimu, Z.; Swain, M.; Santamaria, P.; Yang, Y., Cutting  
30 Edge: CD28 Engagement Releases Antigen-Activated Invariant NKT Cells from the  
31 Inhibitory Effects of PD-1. *J. Immunol.* **2009**, *18*, 6644-6647.

32 44. Spitzer, M. H.; Carmi, Y.; Reticker-Flynn, N. E.; Kwek, S. S.; Madhireddy, D.;  
33 Martins, M. M.; Gherardini, P. F.; Prestwood, T. R.; Chabon, J.; Bendall, S. C.; Fong, L.;  
34 Nolan, G. P.; Engleman, E. G., Systemic Immunity Is Required for Effective Cancer  
35 Immunotherapy. *Cell* **2017**, *168*, 487-502

36 45. Pardi, N.; Hogan, M. J.; Naradikian, M. S.; Parkhouse, K.; Cain, D. W.; Jones, L.;  
37 Moody, M. A.; Verkerke, H. P.; Myles, A.; Willis, E.; LaBranche, C. C.; Montefiori, D. C.;  
38 Lobby, J. L.; Saunders, K. O.; Liao, H. X.; Korber, B. T.; Sutherland, L. L.; Scarce, R. M.;  
39 Hraber, P. T.; Tombacz, I. *et al.*, Nucleoside-Modified mRNA Vaccines Induce Potent T  
40 Follicular Helper and Germinal Center B Cell Responses. *J. Exp. Med.* **2018**, *215*, 1571-1588.

41 46. Im, J. S.; Arora, P.; Bricard, G.; Molano, A.; Venkataswamy, M. M.; Baine, I.; Jerud,  
42 E. S.; Goldberg, M. F.; Baena, A.; Yu, K. O.; Ndonye, R. M.; Howell, A. R.; Yuan, W.;  
43 Cresswell, P.; Chang, Y. T.; Illarionov, P. A.; Besra, G. S.; Porcelli, S. A., Kinetics and  
44 Cellular Site of Glycolipid Loading Control the Outcome of Natural Killer T Cell Activation.  
45 *Immunity* **2009**, *30*, 888-898.

46 47. Torreno-Pina, J. A.; Manzo, C.; Salio, M.; Aichinger, M. C.; Oddone, A.;  
47 Lakadamyali, M.; Shepherd, D.; Besra, G. S.; Cerundolo, V.; Garcia-Parajo, M. F., The Actin  
48 Cytoskeleton Modulates the Activation of iNKT Cells by Segregating CD1d Nanoclusters on  
49 Antigen-Presenting Cells. *Proc. Natl. Acad. Sci. U. S. A.* **2016**, *113*, E772-781.



- 1 48. Nowyhed, H. N.; Chandra, S.; Kiosses, W.; Marcovecchio, P.; Andary, F.; Zhao, M.;  
2 Fitzgerald, M. L.; Kronenberg, M.; Hedrick, C. C., ATP Binding Cassette Transporter  
3 ABCA7 Regulates NKT Cell Development and Function by Controlling CD1d Expression  
4 and Lipid Raft Content. *Sci. Rep.* **2017**, *7*, 40273.
- 5 49. Park, Y. K.; Lee, J. W.; Ko, Y. G.; Hong, S.; Park, S. H., Lipid Rafts Are Required for  
6 Efficient Signal Transduction by CD1d. *Biochem. Biophys. Res. Commun.* **2005**, *327*, 1143-  
7 1154.
- 8 50. Starbeck-Miller, G. R.; Xue, H. H.; Harty, J. T., Il-12 and Type I Interferon Prolong  
9 the Division of Activated CD8 T Cells by Maintaining High-Affinity IL-2 Signaling in Vivo.  
10 *J. Exp. Med.* **2014**, *211*, 105-120.
- 11 51. Murugaiyan, G.; Saha, B., IL-27 in Tumor Immunity and Immunotherapy. *Trends*  
12 *Mol. Med.* **2013**, *19*, 108-116.
- 13 52. Pennock, N. D.; Gapin, L.; Kedl, R. M., IL-27 Is Required for Shaping the Magnitude,  
14 Affinity Distribution, and Memory of T Cells Responding to Subunit Immunization. *Proc.*  
15 *Natl. Acad. Sci. U. S. A.* **2014**, *111*, 16472-16477.
- 16 53. Wei, J.; Xia, S.; Sun, H.; Zhang, S.; Wang, J.; Zhao, H.; Wu, X.; Chen, X.; Hao, J.;  
17 Zhou, X.; Zhu, Z.; Gao, X.; Gao, J. X.; Wang, P.; Wu, Z.; Zhao, L.; Yin, Z., Critical Role of  
18 Dendritic Cell-Derived IL-27 in Antitumor Immunity through Regulating the Recruitment and  
19 Activation of NK and NKT Cells. *J. Immunol.* **2013**, *191*, 500-508.
- 20 54. Semmling, V.; Lukacs-Kornek, V.; Thaiss, C. A.; Quast, T.; Hochheiser, K.; Panzer,  
21 U.; Rossjohn, J.; Perlmutter, P.; Cao, J.; Godfrey, D. I.; Savage, P. B.; Knolle, P. A.; Kolanus,  
22 W.; Forster, I.; Kurts, C., Alternative Cross-Priming through CCL17-CCR4-Mediated  
23 Attraction of CTLs toward NKT Cell-Licensed DCs. *Nat. Immunol.* **2010**, *11*, 313-320.
- 24 55. Gottschalk, C.; Mettke, E.; Kurts, C., The Role of Invariant Natural Killer T Cells in  
25 Dendritic Cell Licensing, Cross-Priming, and Memory CD8(+) T Cell Generation. *Front.*  
26 *Immunol.* **2015**, *6*, 379.
- 27 56. Fotin-Mleczek, M.; Zanzinger, K.; Heidenreich, R.; Lorenz, C.; Thess, A.; Duchardt,  
28 K. M.; Kallen, K. J., Highly Potent mRNA Based Cancer Vaccines Represent an Attractive  
29 Platform for Combination Therapies Supporting an Improved Therapeutic Effect. *J. Gene*  
30 *Med.* **2012**, *14*, 428-439.
- 31 57. Bae, E. A.; Seo, H.; Kim, B. S.; Choi, J.; Jeon, I.; Shin, K. S.; Koh, C. H.; Song, B.;  
32 Kim, I. K.; Min, B. S.; Han, Y. D.; Shin, S. J.; Kang, C. Y., Activation of NKT Cells in an  
33 Anti-PD-1-Resistant Tumor Model Enhances Anti-Tumor Immunity by Reinvigorating  
34 Exhausted CD8 T Cells. *Cancer Res.* **2018**, *78*, 5315-5326
- 35 58. Iyoda, T.; Ushida, M.; Kimura, Y.; Minamino, K.; Hayuka, A.; Yokohata, S.; Ehara,  
36 H.; Inaba, K., Invariant NKT Cell Anergy Is Induced by a Strong TCR-Mediated Signal Plus  
37 Co-Stimulation. *Int. immunol.* **2010**, *22*, 905-913.
- 38 59. Wingender, G.; Birkholz, A. M.; Sag, D.; Farber, E.; Chitale, S.; Howell, A. R.;  
39 Kronenberg, M., Selective Conditions Are Required for the Induction of Invariant NKT Cell  
40 Hyporesponsiveness by Antigenic Stimulation. *J. Immunol.* **2015**, *195*, 3838-3848.
- 41 60. Wilson, M. T.; Johansson, C.; Olivares-Villagomez, D.; Singh, A. K.; Stanic, A. K.;  
42 Wang, C. R.; Joyce, S.; Wick, M. J.; Van Kaer, L., The Response of Natural Killer T Cells to  
43 Glycolipid Antigens Is Characterized by Surface Receptor Down-Modulation and Expansion.  
44 *Proc. Natl. Acad. Sci. U. S. A.* **2003**, *100*, 10913-10918.
- 45 61. Durgan, K.; Ali, M.; Warner, P.; Latchman, Y. E., Targeting NKT Cells and PD-L1  
46 Pathway Results in Augmented Anti-Tumor Responses in a Melanoma Model. *Cancer*  
47 *Immunol. Immunother. CII* **2011**, *60*, 547-558.
- 48 62. Sayour, E. J.; Grippin, A.; De Leon, G.; Stover, B.; Rahman, M.; Karachi, A.;  
49 Wummer, B.; Moore, G.; Castillo-Caro, P.; Fredenburg, K.; Sarkisian, M. R.; Huang, J.;  
50 Deleyrolle, L. P.; Sahay, B.; Carrera-Justiz, S.; Mendez-Gomez, H. R.; Mitchell, D. A.,

- 1 Personalized Tumor RNA Loaded Lipid-Nanoparticles Prime the Systemic and Intratumoral  
2 Milieu for Response to Cancer Immunotherapy. *Nano Lett.* **2018**, *18*, 6195-6206.
- 3 63. Tang, H.; Liang, Y.; Anders, R. A.; Taube, J. M.; Qiu, X.; Mulgaonkar, A.; Liu, X.;  
4 Harrington, S. M.; Guo, J.; Xin, Y.; Xiong, Y.; Nham, K.; Silvers, W.; Hao, G.; Sun, X.;  
5 Chen, M.; Hannan, R.; Qiao, J.; Dong, H.; Peng, H. *et al.*, PD-L1 on Host Cells Is Essential  
6 for PD-L1 Blockade-Mediated Tumor Regression. *J Clin. Invest.* **2018**, *128*, 580-588.
- 7 64. Garris, C. S.; Arlauckas, S. P.; Kohler, R. H.; Trefny, M. P.; Garren, S.; Piot, C.;  
8 Engblom, C.; Pfirschke, C.; Siwicki, M.; Gungabeesoon, J.; Freeman, G. J.; Warren, S. E.;  
9 Ong, S.; Browning, E.; Twitty, C. G.; Pierce, R. H.; Le, M. H.; Algazi, A. P.; Daud, A. I.; Pai,  
10 S. I. *et al.*, Successful Anti-PD-1 Cancer Immunotherapy Requires T Cell-Dendritic Cell  
11 Crosstalk Involving the Cytokines IFN- $\gamma$  and IL-12. *Immunity* **2018**, *49*, 1148-1161
- 12 65. Huang, J. R.; Tsai, Y. C.; Chang, Y. J.; Wu, J. C.; Hung, J. T.; Lin, K. H.; Wong, C.  
13 H.; Yu, A. L., Alpha-Galactosylceramide but Not Phenyl-Glycolipids Induced NKT Cell  
14 Anergy and IL-33-Mediated Myeloid-Derived Suppressor Cell Accumulation *via*  
15 Upregulation of Egr2/3. *J. Immunol.* **2014**, *192*, 1972-1981.
- 16 66. Kojo, S.; Elly, C.; Harada, Y.; Langdon, W. Y.; Kronenberg, M.; Liu, Y. C.,  
17 Mechanisms of Nkt Cell Anergy Induction Involve Cbl-B-Promoted Monoubiquitination of  
18 CARMA1. *Proc. Natl. Acad. Sci. U. S. A.* **2009**, *106*, 17847-17851.
- 19 67. Kling, J. C.; Jordan, M. A.; Pitt, L. A.; Meiners, J.; Thanh-Tran, T.; Tran, L. S.;  
20 Nguyen, T. T. K.; Mittal, D.; Villani, R.; Steptoe, R. J.; Khosrotehrani, K.; Berzins, S. P.;  
21 Baxter, A. G.; Godfrey, D. I.; Blumenthal, A., Temporal Regulation of Natural Killer T Cell  
22 Interferon Gamma Responses by Beta-Catenin-Dependent and -Independent Wnt Signaling.  
23 *Front. Immunol.* **2018**, *9*, 483.
- 24 68. Berga-Bolaños, R.; Sharma, A.; Steinke, F. C.; Pyaram, K.; Kim, Y. H.; Sultana, D.  
25 A.; Fang, J. X.; Chang, C. H.; Xue, H. H.; Heller, N. M.; Sen, J. M.,  $\beta$ -Catenin Is Required for  
26 the Differentiation of iNKT2 and iNKT17 Cells That Augment IL-25-Dependent Lung  
27 Inflammation. *BMC Immunol.* **2015**, *16*, 62.
- 28 69. Metelitsa, L. S., Anti-Tumor Potential of Type-I NKT Cells against CD1d-Positive  
29 and CD1d-Negative Tumors in Humans. *Clin. Immunol.* **2011**, *140*, 119-129.
- 30 70. Favreau, M.; Vanderkerken, K.; Elewaut, D.; Venken, K.; Menu, E., Does an NKT-  
31 Cell-Based Immunotherapeutic Approach Have a Future in Multiple Myeloma? *Oncotarget*  
32 **2016**, *7*, 23128-23140.
- 33 71. Lam, P. Y.; Nissen, M. D.; Mattarollo, S. R., Invariant Natural Killer T Cells in  
34 Immune Regulation of Blood Cancers: Harnessing Their Potential in Immunotherapies. *Front.*  
35 *Immunol.* **2017**, *8*, 1355.
- 36 72. Van Meirvenne, S.; Straetman, L.; Heirman, C.; Dullaers, M.; De Greef, C.; Van  
37 Tendeloo, V.; Thielemans, K., Efficient Genetic Modification of Murine Dendritic Cells by  
38 Electroporation with mRNA. *Cancer Gene Ther.* **2002**, *9*, 787-797.
- 39 73. Oliver Plettenburg, O.; Bodmer-Narkevitch, V.; Wong, C., Synthesis of  $\alpha$ -Galactosyl  
40 Ceramide, a Potent Immunostimulatory Agent. *J. Org. Chem.* **2002**, *67*, 4559-4564.

41